



Independent Microevolution Mediated by Mobile Genetic Elements of Individual *Clostridium difficile* Isolates from Clade 4 Revealed by Whole-Genome Sequencing

Yuan Wu,^{a,b} Chen Liu,^c Wen-Ge Li,^a Jun-Li Xu,^c Wen-Zhu Zhang,^a Yi-Fei Dai,^c Jin-Xing Lu^{a,b}

^aState Key Laboratory of Infectious Disease Prevention and Control, National Institute for Communicable Disease Control and Prevention, Chinese Center for Disease Control and Prevention, Beijing, China

^bCollaborative Innovation Center for Diagnosis and Treatment of Infectious Diseases, Hangzhou, China

^cNovogene Bioinformatics Institute, Beijing, China

ABSTRACT Horizontal gene transfer of mobile genetic elements (MGEs) accounts for the mosaic genome of *Clostridium difficile*, leading to acquisition of new phenotypes, including drug resistance and reconstruction of the genomes. MGEs were analyzed according to the whole-genome sequences of 37 *C. difficile* isolates with a variety of sequence types (STs) within clade 4 from China. Great diversity was found in each transposon even within isolates with the same ST. Two novel transposons were identified in isolates ZR9 and ZR18, of which approximately one third to half of the genes showed heterogenous origins compared with the usual intestinal bacterial genes. Most importantly, *catD*, known to be harbored by Tn4453a/b, was replaced by *aac(6')* *aph(2'')* in isolates 2, 7, and 28. This phenomenon illustrated the frequent occurrence of gene exchanges between *C. difficile* and other enterobacteria with individual heterogeneity. Numerous prophages and CRISPR arrays were identified in *C. difficile* isolates of clade 4. Approximately 20% of spacers were located in prophage-carried CRISPR arrays, providing a new method for typing and tracing the origins of closely related isolates, as well as in-depth studies of the mechanism underlying genome remodeling. The rates of drug resistance were obviously higher than those reported previously around the world, although all isolates retained high sensitivity to vancomycin and metronidazole. The increasing number of *C. difficile* isolates resistant to all antibiotics tested here suggests the ease with which resistance is acquired *in vivo*. This study gives insights into the genetic mechanism of microevolution within clade 4.

IMPORTANCE Mobile genetic elements play a key role in the continuing evolution of *Clostridium difficile*, resulting in the emergence of new phenotypes for individual isolates. On the basis of whole-genome sequencing analysis, we comprehensively explored transposons, CRISPR, prophage, and genetic sites for drug resistance within clade 4 *C. difficile* isolates with different sequence types. Great diversity in MGEs and a high rate of multidrug resistance were found within this clade, including new transposons, Tn4453a/b with *aac(6')* *aph(2'')* instead of *catD*, and a relatively high rate of prophage-carried CRISPR arrays. These findings provide important new insights into the mechanism of genome remodeling within clade 4 and offer a new method for typing and tracing the origins of closely related isolates.

KEYWORDS *Clostridium difficile*, antifungal resistance, horizontal gene transfer, microevolution, mobile genetic elements

Clostridium difficile, a Gram-positive, anaerobic bacterium, has emerged as the leading cause of antimicrobial and health care-associated diarrhea in humans (1). *C. difficile* is widespread in the environment and the gastrointestinal tracts of humans and

Citation Wu Y, Liu C, Li W-G, Xu J-L, Zhang W-Z, Dai Y-F, Lu J-X. 2019. Independent microevolution mediated by mobile genetic elements of individual *Clostridium difficile* isolates from clade 4 revealed by whole-genome sequencing. *mSystems* 4:e00252-18. <https://doi.org/10.1128/mSystems.00252-18>.

Editor Sergio Baranzini, University of California, San Francisco

Copyright © 2019 Wu et al. This is an open-access article distributed under the terms of the [Creative Commons Attribution 4.0 International license](https://creativecommons.org/licenses/by/4.0/).

Address correspondence to Jin-Xing Lu, lujinxing@icdc.cn.

Y.W. and C.L. contributed equally to this study.

Received 11 October 2018

Accepted 18 January 2019

Published 26 March 2019

animals (2). CD630, which was the first fully sequenced and annotated closed genome of *C. difficile*, comprises a large circular chromosome of 4.3 Mb, with low GC content (29.06%) (3, 4). Subsequently, thousands of whole-genome sequences (WGS) of *C. difficile* were published, with sizes ranging from 4.1 to 4.3 Mb (5–7). The high proportion (about 11% in strain 630) of mobile genetic elements (MGEs) contributes to the remarkable dynamic and mosaic genome of *C. difficile* (8). The MGEs include transposable and conjugative elements, plasmids, bacteriophages, insertion sequences (IS), clustered regularly interspersed short palindromic repeat (CRISPR) elements, group I introns, and *sigK* intervening (skin) elements (9, 10). These elements play a role in horizontal gene transfer (HGT) between distinct *C. difficile* isolates and between *C. difficile* and other intestinal pathogens, such as *Enterococcus faecalis*, and *Enterococcus faecium* (9, 11–13).

According to the multilocus sequence typing (MLST) scheme established by Griffiths et al. (14), five distinct phylogenetic lineages (clades 1 to 5) are widely recognized, and an additional clade, clade C-I, was identified, which was confirmed by WGS studies (15–17). Clade 1 is highly heterogeneous and includes many clinically significant toxigenic and nontoxigenic MLST sequence types (STs) and PCR ribotypes (RTs), such as RTs 014, 002, and 018 and STs 2, 14, and 49 (18, 19). A representative of clade 2 is hypervirulent RT027, which has caused severe outbreaks, especially in Europe and North America (20–23). Within clade 3, RT023 and STs 5 and 22 were isolated from humans in Europe (18, 24). In clade 4, RT017 (ST37) has been associated with outbreaks in Europe (25, 26) and North America (27) and is responsible for most *C. difficile* infections (CDIs) in Asia (28). In addition, RT017 is often clindamycin and fluoroquinolone resistant. Clade 5 contains not only RT078 but also RTs 033, 045, 066, 126, 127, 237, 280, 281, and 288 from a diverse collection of clinical, animal, and food sources worldwide and also demonstrates great heterogeneity (29, 30).

In this study, the WGS of 37 clinical *C. difficile* isolates from clade 4 with divergent origins in China were obtained, annotated, and analyzed. The genomic regions encoding toxins A and B (PaLoc) and the binary toxin (CdtLoc), MGEs and molecular typing (MLST and PCR ribotyping) were compared and analyzed systematically based on the WGS data. In addition, antibiotic resistance genes, putative resistance point mutation sites, and the relationship with the results of drug susceptibility tests were evaluated. These results will further our knowledge of the genetic characterization of clade 4 and further elucidate the role of MGEs in the evolution, pathogenicity, and transfer of drug resistance genes and toxin-related genes of *C. difficile*.

RESULTS

Genomic characteristics and population structure in clade 4. Details of the genome sizes of these 37 *C. difficile* isolates (range from 3.9 to 4.3 Mb), and other common features are summarized in Table S1 in the supplemental material. The population structure of clade 4 based on the neighbor-joining (N-J) phylogenetic tree correlated well with groups defined according to MLST, PCR ribotyping, and toxin profile but showed no obvious correlation with geographic distribution (Fig. 1). RT017 had two distinct sublineages, ST37 and ST81 (Fig. 1). Each ST cluster was highly conserved, although within the ST37 cluster, ZR18 displayed obvious distinctions compared with the rest of the ST37 isolates (Fig. 1). In the subsequent analysis, we explored the reasons for these distinctions at the genomic level. ST332 was a novel ST that we identified with a unique positive *tcdA* gene, which formed a singleton in the N-J tree (Fig. 1). Two nontoxigenic isolates (ST109 and ST39) also spread as singletons (Fig. 1).

Genetic diversity of MGEs in clade 4 (transposons, prophages, CRISPRs, and plasmids). (i) **Transposons and conjugative transposons.** Several transposons (Tns) and conjugative transposons (CTNs), including CTn5, Tn4453a/b, Tn5397, Tn5398, Tn6194, Tn916, and novel putative transposons containing regions homologous with CTn2 and CTn7 (Table 1), were identified by comparison with reference genomes. A novel putative transposon element was discovered in isolate ZR9. This element was

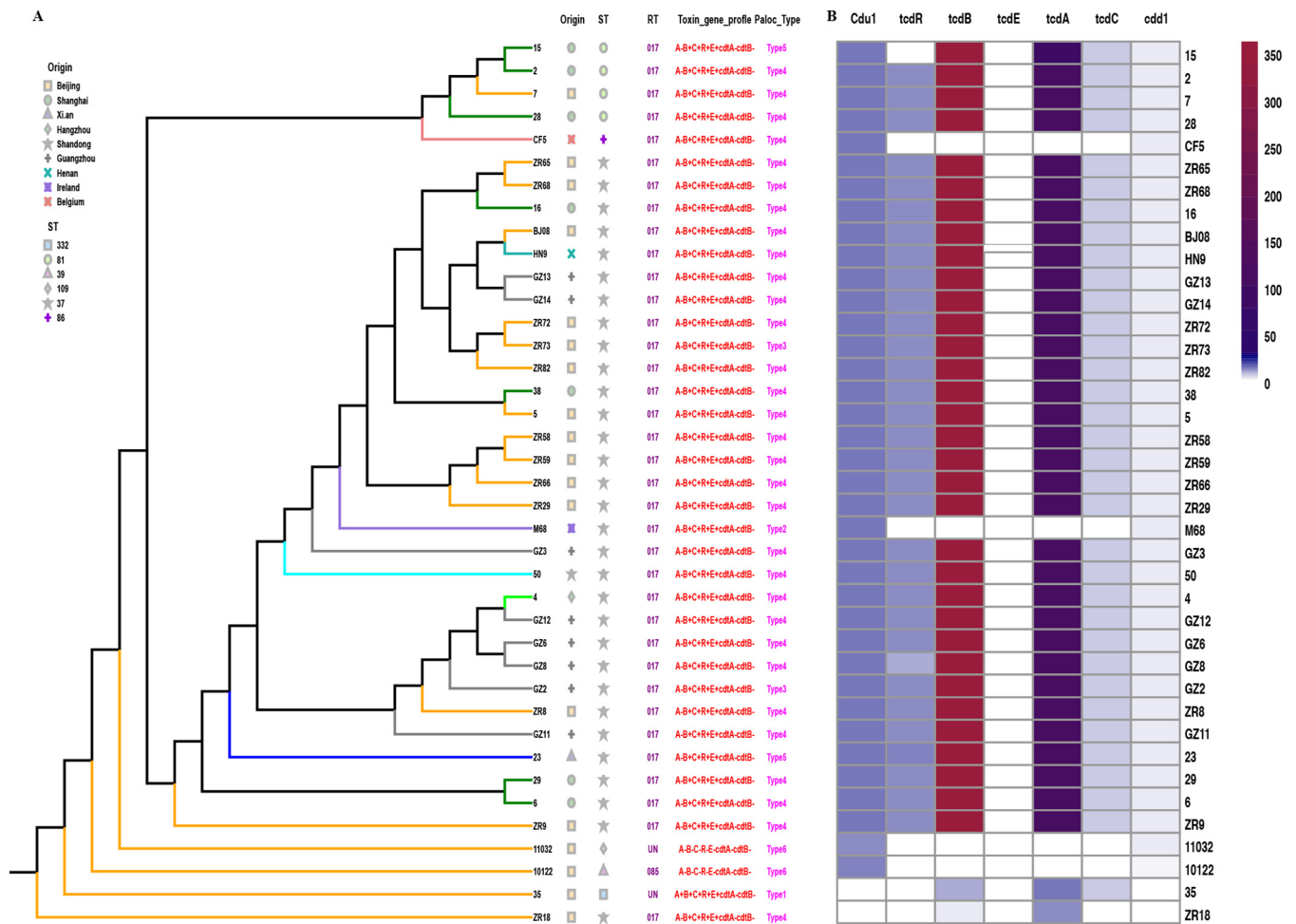


FIG 1 Population structure of clade 4 based on the neighbor-joining (N-J) phylogenetic tree and single nucleotide polymorphisms in the PaLoc of all tested isolates. (A) N-J tree of 37 *C. difficile* isolates with diverse origins and STs. (B) SNPs identified within the PaLoc of *C. difficile* isolates.

located in scaffold 35 from 2,689 to 3,4943 bp and contained 36 coding sequences (CDS), of which 10 were unique in this element, while the remaining 26 genes demonstrated 83.33% to 100% identity with CTn2 (Fig. 2A). Among the 10 unique genes, G002737, G002739, G002743, G002760, and G002761 were annotated as *C. difficile* putative conjugative transposon protein Tn1549-like, CTn2-ORF30, CTn2-ORF32, CTn5 ORF2, 18, and 19, respectively. G002741 was annotated as putative RNA methyltransferase of *C. difficile* E7. G002744, G002747, G002748, and G002759 were defined as hypothetical protein, bacterial regulatory helix (AraC family protein), transcriptional regulator (effector binding domain protein), and transcriptional regulator (AbrB family domain protein), respectively. In isolate ZR18, another putative novel mobile element was found, including 24 coding sequences, of which 10 genes were absent in CTn7, while the other genes were similar to those in CTn7 (Fig. 3A). Large fragment insertions and deletions located in 630_03693 to 630_03688, and 630_03686 to *mgtA2* were identified in isolate ZR18 (Fig. 3A). The 10 novel genes (G001824, G001827, G001828, G001967, G001969, G001972, G001974, G001975, G001976, and G001977) in ZR18 were annotated as hypothetical protein, CTn7-ORF 4, 6, and conjugal transfer protein of *C. difficile*, and also proteins of other gut pathogens such as *Firmicutes* and *Enterococcus faecium*. In addition, a CTn7-like element was identified in reference M68, showing >85% identity with 630 CTn7 (Fig. 3A). Two genes (M68GM003529 and M68GM003530) were inserted between 630_03695 and 630_03694. In M68, M68GM003535 replaced 630_03690 at the same site, while 630_03685 was missing (Fig. 3A). It is noteworthy

TABLE 1 General description of 37 *C. difficile* isolates in this study

Isolate	Origin	ST	RT	Toxin gene profile	Tn ^a	Potential plasmid sequence	No. of prophages ^b
35	Beijing	332	UN	A ⁺ B ⁺ C ⁺ R ⁺ E ⁺ cdtA ⁻ cdtB ⁻	Tn5398-like	1	7
2	Shanghai	81	017	A ⁻ B ⁺ C ⁺ R ⁺ E ⁺ cdtA ⁻ cdtB ⁻	CTn5-like, Tn4453a/b, Tn5397-like, Tn6194-like	14	11
28	Shanghai	81	017	A ⁻ B ⁺ C ⁺ R ⁺ E ⁺ cdtA ⁻ cdtB ⁻	CTn5-like, Tn4453a/b, Tn5397-like, Tn5398-like, Tn6194-like	13	7
7	Beijing	81	017	A ⁻ B ⁺ C ⁺ R ⁺ E ⁺ cdtA ⁻ cdtB ⁻	CTn5-like, Tn4453a/b, Tn5397-like, Tn5398-like, Tn6194-like	14	8
15	Shanghai	81	017	A ⁻ B ⁺ C ⁺ R ⁺ E ⁺ cdtA ⁻ cdtB ⁻	CTn5-like, Tn5398-like	4	9
10122	Beijing	39	085	A ⁻ B ⁻ C ⁻ R ⁻ E ⁻ cdtA ⁻ cdtB ⁻	CTn5-like	5	5
11032	Beijing	109	UN	A ⁻ B ⁻ C ⁻ R ⁻ E ⁻ cdtA ⁻ cdtB ⁻		4	3
16	Shanghai	37	017	A ⁻ B ⁺ C ⁺ R ⁺ E ⁺ cdtA ⁻ cdtB ⁻	CTn5-like, Tn5398-like, Tn6194-like	9	8
23	Xi'an	37	017	A ⁻ B ⁺ C ⁺ R ⁺ E ⁺ cdtA ⁻ cdtB ⁻	CTn5-like, Tn5397-like, Tn5398-like, Tn6194-like	5	7
29	Shanghai	37	017	A ⁻ B ⁺ C ⁺ R ⁺ E ⁺ cdtA ⁻ cdtB ⁻	CTn5-like, Tn5397-like, Tn5398-like, Tn6194-like	10	6
38	Shanghai	37	017	A ⁻ B ⁺ C ⁺ R ⁺ E ⁺ cdtA ⁻ cdtB ⁻	CTn5-like, Tn5397-like, Tn6194-like	14	8
4	Hangzhou	37	017	A ⁻ B ⁺ C ⁺ R ⁺ E ⁺ cdtA ⁻ cdtB ⁻	CTn5-like, Tn5397-like, Tn5398-like, Tn6194-like	10	8
5	Beijing	37	017	A ⁻ B ⁺ C ⁺ R ⁺ E ⁺ cdtA ⁻ cdtB ⁻	CTn5-like, Tn5397-like, Tn5398-like, Tn6194-like	13	9
50	Shandong	37	017	A ⁻ B ⁺ C ⁺ R ⁺ E ⁺ cdtA ⁻ cdtB ⁻	CTn5-like, Tn5398-like	1	5
6	Shanghai	37	017	A ⁻ B ⁺ C ⁺ R ⁺ E ⁺ cdtA ⁻ cdtB ⁻	CTn5-like, Tn5397-like, Tn5398-like, Tn6194-like	10	7
BJ08	Beijing	37	017	A ⁻ B ⁺ C ⁺ R ⁺ E ⁺ cdtA ⁻ cdtB ⁻	CTn5-like, Tn5397-like, Tn5398-like	9	7
GZ2	Guangzhou	37	017	A ⁻ B ⁺ C ⁺ R ⁺ E ⁺ cdtA ⁻ cdtB ⁻	CTn5-like, Tn5397-like, Tn5398-like, Tn6194-like	10	7
GZ3	Guangzhou	37	017	A ⁻ B ⁺ C ⁺ R ⁺ E ⁺ cdtA ⁻ cdtB ⁻	CTn5-like, Tn5397-like, Tn6194-like	10	8
GZ6	Guangzhou	37	017	A ⁻ B ⁺ C ⁺ R ⁺ E ⁺ cdtA ⁻ cdtB ⁻	CTn5-like, Tn5397-like, Tn5398-like, Tn6194-like	10	8
GZ8	Guangzhou	37	017	A ⁻ B ⁺ C ⁺ R ⁺ E ⁺ cdtA ⁻ cdtB ⁻	CTn5-like, Tn5397-like	10	9
GZ11	Guangzhou	37	017	A ⁻ B ⁺ C ⁺ R ⁺ E ⁺ cdtA ⁻ cdtB ⁻	CTn5-like, Tn5397-like, Tn6194-like	11	8
GZ12	Guangzhou	37	017	A ⁻ B ⁺ C ⁺ R ⁺ E ⁺ cdtA ⁻ cdtB ⁻	CTn5-like, Tn5397-like, Tn6194-like	10	7
GZ13	Guangzhou	37	017	A ⁻ B ⁺ C ⁺ R ⁺ E ⁺ cdtA ⁻ cdtB ⁻	CTn5-like, Tn5397-like, Tn5398-like, Tn6194-like	13	9
GZ14	Guangzhou	37	017	A ⁻ B ⁺ C ⁺ R ⁺ E ⁺ cdtA ⁻ cdtB ⁻	CTn5-like, Tn5397-like, Tn5398-like, Tn6194-like	13	11
ZR58	Beijing	37	017	A ⁻ B ⁺ C ⁺ R ⁺ E ⁺ cdtA ⁻ cdtB ⁻	CTn5-like, Tn5397-like, Tn6194-like	14	11
ZR59	Beijing	37	017	A ⁻ B ⁺ C ⁺ R ⁺ E ⁺ cdtA ⁻ cdtB ⁻	CTn5-like, Tn5397-like, Tn6194-like	14	13
ZR65	Beijing	37	017	A ⁻ B ⁺ C ⁺ R ⁺ E ⁺ cdtA ⁻ cdtB ⁻	CTn5-like, Tn5398-like	4	8
ZR66	Beijing	37	017	A ⁻ B ⁺ C ⁺ R ⁺ E ⁺ cdtA ⁻ cdtB ⁻	CTn5-like, Tn5397-like, Tn5398-like, Tn6194-like	14	13
ZR68	Beijing	37	017	A ⁻ B ⁺ C ⁺ R ⁺ E ⁺ cdtA ⁻ cdtB ⁻	CTn5-like, Tn5398-like	5	8
ZR72	Beijing	37	017	A ⁻ B ⁺ C ⁺ R ⁺ E ⁺ cdtA ⁻ cdtB ⁻	CTn5-like, Tn5397-like, Tn5398-like	9	8
ZR73	Beijing	37	017	A ⁻ B ⁺ C ⁺ R ⁺ E ⁺ cdtA ⁻ cdtB ⁻	CTn5-like, Tn5397-like, Tn5398-like	8	10
ZR82	Beijing	37	017	A ⁻ B ⁺ C ⁺ R ⁺ E ⁺ cdtA ⁻ cdtB ⁻	CTn5-like, Tn5397-like, Tn5398-like	8	7
ZR29	Beijing	37	017	A ⁻ B ⁺ C ⁺ R ⁺ E ⁺ cdtA ⁻ cdtB ⁻	CTn5-like, Tn5397-like, Tn5398-like, Tn6194-like	14	9
ZR18	Beijing	37	017	A ⁻ B ⁺ C ⁺ R ⁺ E ⁺ cdtA ⁻ cdtB ⁻	CTn5-like, npe-CTn7, Tn4453a/b, Tn5397-like	7	5
ZR8	Beijing	37	017	A ⁻ B ⁺ C ⁺ R ⁺ E ⁺ cdtA ⁻ cdtB ⁻	CTn5-like, Tn5397-like, Tn5398-like, Tn6194-like	10	6
ZR9	Beijing	37	017	A ⁻ B ⁺ C ⁺ R ⁺ E ⁺ cdtA ⁻ cdtB ⁻	npe-CTn2, Tn5397-like, Tn6194-like	9	6
HN9	Henan	37	017	A ⁻ B ⁺ C ⁺ R ⁺ E ⁺ cdtA ⁻ cdtB ⁻	CTn5-like, Tn5397-like, Tn5398-like	9	8
CD630		54	012	A ⁺ B ⁺ C ⁺ R ⁺ E ⁺ cdtA ⁻ cdtB ⁻			
M68	Ireland	37	017	A ⁻ B ⁺ C ⁺ R ⁺ E ⁺ cdtA ⁻ cdtB ⁻	CTn5-like, CTn7-like, Tn5397-like		
CF5	Belgium	86	017	A ⁻ B ⁺ C ⁺ R ⁺ E ⁺ cdtA ⁻ cdtB ⁻	CTn5-like		

^anpe, novel putative element.

^bTotal number of incomplete, intact, and questionable prophage.

that nearly half of genes in CTn7 were lost in M68, with the addition of another 11 coding genes (Fig. 3A), encoding transcriptional regulator, ABC transporter, antimicrobial resistance gene *ermB* (M68GM003552), and *bcrA* (M68GM003544), putative truncated zeta protein, ATPase-associated proteins, and other genes originating from *C. difficile* and other enteric bacteria (*Erysipelotrichaceae*, *E. faecalis*, *E. faecium*, *Campylobacter jejuni*, *Firmicutes*, and *Staphylococcus aureus*).

CTn5-like transposons, belonging to the Tn1549 family, were detected widely in the tested *C. difficile* isolates of clade 4, with the exception of isolate 35 and 11032 (Fig. 2B). Ten types were divided according to gene composition as follows (Fig. 2B): type 1 (HN9), type 2 (BJ08), type 3 (15), type 4 (GZ8), type 5 (ZR18), type 6 (GZ3), type 7 (29), type 8 (2, 28, 5, 7, ZR8, ZR9), type 9 (23, 38, 4, 50, 6, GZ11, GZ12, GZ2, GZ6, ZR29, ZR58, ZR59, Z566, 10122), and type 10 (16, GZ13, GZ14, ZR65, ZR68, ZR72, ZR73, ZR82). Two common major deletions in the conjugative region were observed in these 10 types, one being a deletion of 630_02052, and the other one located between 630_02066 and 630_02072 (Fig. 2B). Especially for types 3, 5, and 8, other large fragment deletions were also discovered in the conjugative region (Fig. 2B).

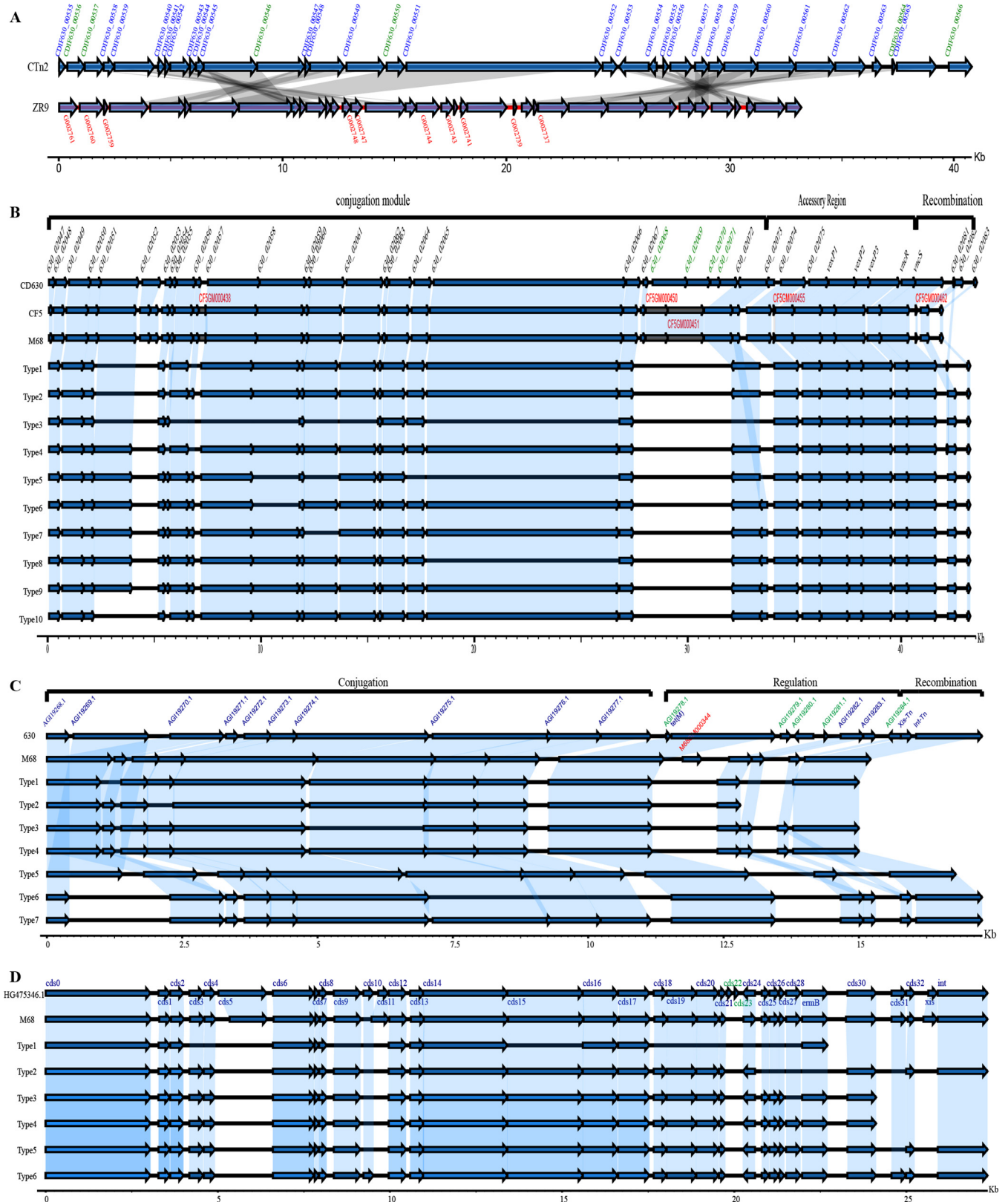


FIG 2 Schematic representation and comparisons of CTn2, CTn5, Tn916, and Tn6194 in target isolates. Blue arrows indicate homologous genes. ORF names in red are unique in related isolates, and ORF names in green are unique to the reference isolates. Regions of homology among isolates are indicated by gray (A) and light blue shading (B to D). (A) Schematic comparisons of CTn2 and new putative Tn in ZR9. (B to D) Schematic comparisons of different types of CTn5 (B), Tn916 (C), and Tn6194 (D).

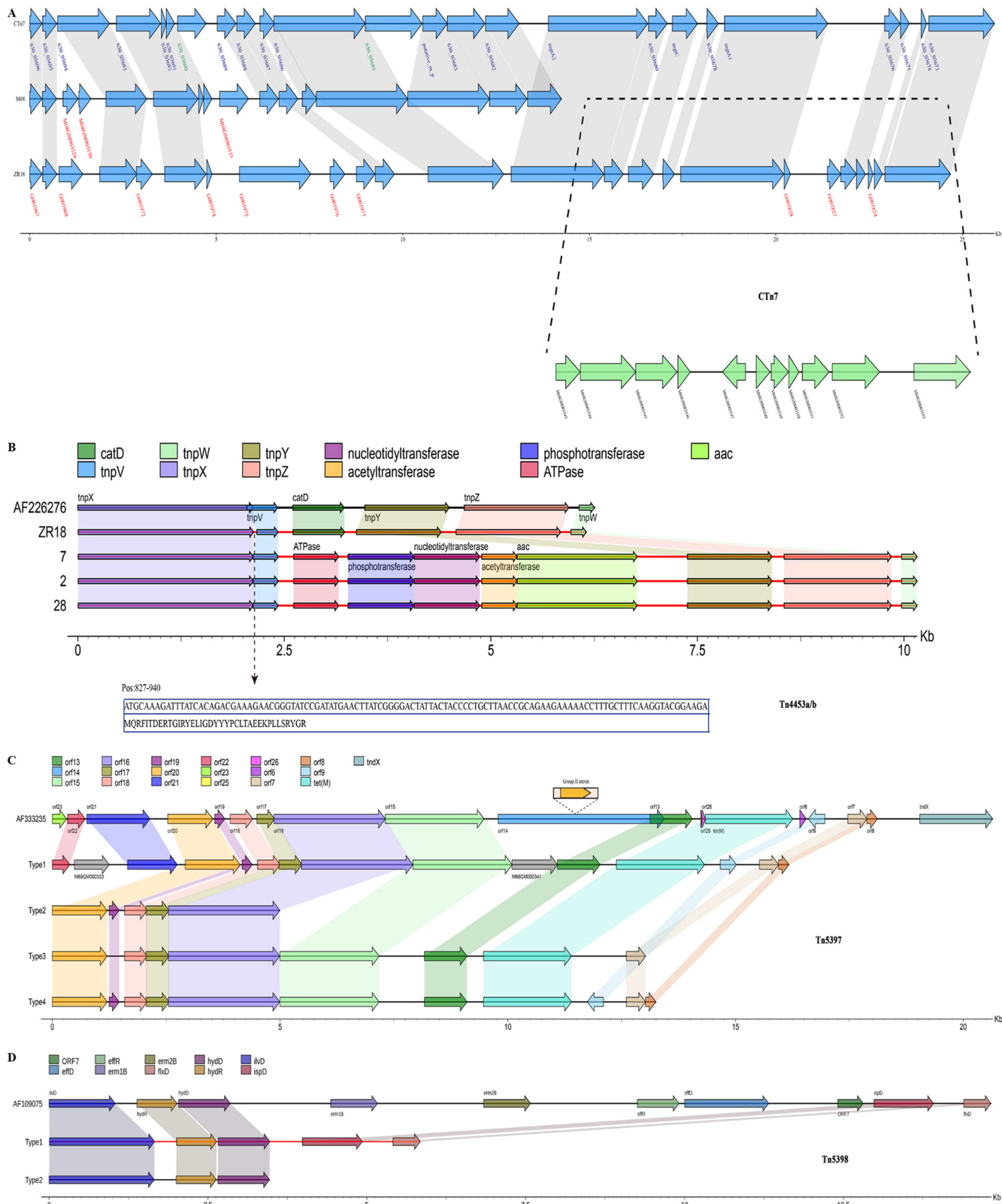


FIG 3 Schematic representation and comparisons of CTn7, Tn4453a/b, Tn5397, and Tn5398 in target isolates. (A) For CTn7, blue arrows refer to homologous genes. ORF names in red are unique in related isolates, and ORF names in green are unique to reference isolates. Regions of homology among isolates are indicated by gray shading. The missing genes of M68 are displayed in regions between the dashed lines in green. For the remaining Tns, different ORFs are represented by distinct colors, and homologous regions are shown in related colors. (B) In Tn4453a/b, the deleted fragment (amino acids and nucleotides) in the *tnpV* gene is indicated in the dark blue box below the dashed arrow line. (C and D) Schematic comparisons of different types of Tn5397 (C) and Tn5398 (D).

Tn4453a/b was found with typical gene organization in isolates ZR18, 2, 7, and 28 (Fig. 3B). The composition and location of genes in ZR18 was identical to that in reference Tn4453a/b, with the exception of a –114-bp deletion in *tnpV* (Fig. 3B). The key feature of this element was the presence of *catD*, which mediates resistance to chloramphenicol. Interestingly, *catD* was absent in isolates 2, 7, and 28 and replaced by five new genes: aminoglycoside acetyltransferase (*aac*), three transferases (phosphotransferase, nucleotidyltransferase, and acetyltransferase) and an ATPase (Fig. 3B). The *aac* gene, which confers resistance to aminoglycoside antibiotics, such as gentamicin, tobramycin, and netilmicin has been widely reported in *Enterococcus* and *Enterobacter*, and can be transferred between Gram-positive and Gram-negative bacteria by transposons (Tn5281, Tn4001, and IS256) or plasmids (31). BLAST analysis revealed that the DNA sequences of *aac* in isolates 2, 7, and 28 showed 100% coverage and identity with *aac(6')* *aph(2'')* in *C. jejuni*. The total length of the gene was 1,455 bp, encoding a bifunctional aminoglycoside *N*-acetyltransferase and aminoglycoside phosphotransferase, which is one of the aminoglycoside-modified enzymes (AMEs), playing critical role in high-level gentamicin-resistant (HLGR) of *Enterococcus* (32).

Tn5397, also known as CTn3 in CD630, was recognized in most isolates in this study and was classified into four types as follows: type 1, ZR18 and M68; type 2, ZR73 and 5; type 3, BJ08, GZ8, and HN9; type 4, ZR82, ZR9, 2, 23, 28, 29, 38, 4, 6, 7, GZ11, GZ12, GZ13, GZ14, GZ2, GZ3, GZ6, ZR29, ZR58, ZR59, ZR66, ZR72, and ZR8 (Table 1). The *tndX* gene, encoding a large serine recombinase, which is essential for insertion/excision of Tn5397, was absent in all types (Fig. 3C). Furthermore, a group II intron within *orf14* was also deleted (Fig. 3C). Significantly, in type 2, Tn5397 was missing some of the downstream genes, including an antimicrobial resistance gene *tetM*, compared with the reference Tn5397 (Fig. 3C). Type 1 displayed the most similar gene composition and structure compared with the reference Tn5397, although two new genes were inserted (Fig. 3C).

Tn5398, first reported in strain 630, contains *erm 1B* and *erm 2B*, and can be transferred between *C. difficile* isolates, or between *C. difficile* and *S. aureus* or *Bacillus subtilis* (33). Two types of Tn5398-like elements were identified here, in which *erm 1B* and *erm 2B* genes were absent (Fig. 3D). Type 1 consisted of 35, ZR73, ZR82, 16, 23, 28, 29, 4, 5, 50, 6, 7, BJ08, GZ13, GZ14, GZ2, GZ6, HN9, ZR29, ZR65, ZR66, ZR68, ZR72, and ZR8, while type 2 was represented only by isolate 15 (Table 1).

Tn916 is a major family transposon reported in *C. difficile* and carries the *tetM* resistance gene. The Tn916 element of these tested isolates were subdivided into multiple types as follows: type 1, GZ8; type 2, ZR18; type 3, ZR73; type 4, 23, 29, 4, 6, GZ11, GZ12, GZ13, GZ14, GZ2, GZ3, GZ6, ZR72, ZR8, ZR82, and ZR9; type 5, BJ08 and HN9; type 6, 5; type 7, 2, 28, 38, 7, ZR29, ZR58, ZR59, and ZR66 (Table 1). The *tetM* resistance and *int* gene (responsible for Tn insertion), which are responsible for insertion, appeared in all types (Fig. 2C). With the exception of type 6 with deletions in three large regions, deletions occurred in a single area of the regulation region in all the other types (Fig. 2C). Intact *xis* and *int* genes were retained in types 3, 4, 6, and 7. The conjugative region was highly homologous within most types, except for types 3, 6, and 7, which had large fragment deletions (Fig. 2C). Isolate ZR18 carried no typical *xis* and *int* genes of Tn916, while BJ08, GZ8, and HN9 contain *int* without *xis*.

The representative gene cluster of Tn6194 carrying *ermB* of strain CII7 (GenBank accession no. [HG475346](#)) was used as a reference in this study. Tn6194 has a conjugation region that is closely related to that of Tn916 but contains an accessory region that is related to Tn5398. M68 demonstrated high-level homology with only the absence of *cds22* and *cds 23*, and indels within *cds5* and *cds 11*, while intact *xis* and *int* genes were retained for excision and insertion (Fig. 2D). The following six types were defined here: type 1, 16, 2, 28, 38, 5, 7, GZ13, and GZ14; type 2, 23; type 3, ZR66; type 4, ZR29, ZR58, and ZR59; type 5, 29, 4, 6, GZ11, GZ12, GZ2, GZ6, ZR8, and ZR9; type 6, GZ3 (Table 1). The *ermB* gene was present in all types except type 2 (Fig. 2D). The *xis* gene, which is involved in the excision of Tn916 from the donated strain were deleted in all types

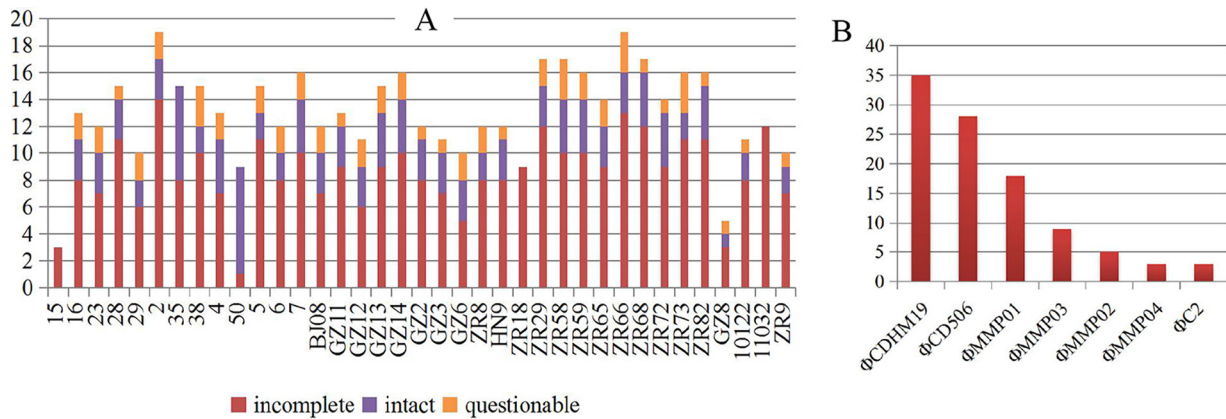


FIG 4 Prophage analysis of 37 *C. difficile* isolates from clade 4. (A) Details of the prophages in each isolate. (B) The most predominant prophages identified in clade 4. Isolates or prophages are shown on the x axes, and the number of prophages is shown on the y axes.

(Fig. 2D). The *int* gene, which plays a key role in the integration of Tn916 into the recipient isolate, appeared in types 2, 5, and 6 only (Fig. 2D).

(ii) Prophages, plasmids, and CRISPR. Prophages were identified in various amounts in all tested isolates (Table S2). In total, 497 prophages were predicted in this study. Isolates 2 and ZR66 contained the highest number of prophages (19 prophages), while isolate 15 had the fewest (3 prophages) (Table S2 and Fig. 4A). A total of 115 intact prophages was confirmed among in all the isolates, except ZR18, 15, and 11032 (Fig. 4A). Among the intact prophages, the number of ΦCDHM19, ΦCD506, ΦMMP01, ΦMMP03, ΦMMP02, ΦMMP04, and ΦC2 was more than three per isolate (Fig. 4B). ΦCDHM19 and ΦCD506 represented more than half (54.78%) of all intact prophages (Fig. 4B). All of these prophages belonged to the *Myoviridae* family, and some were induced during *C. difficile* infection (34). Most prophages identified here were homologous to known phages reported in *C. difficile*, although a few were similar to other bacterial phages, such as *C. jejuni*, *S. aureus*, *Enterobacteria*, *Bacillus*, and other unusual bacteria, such as *Prochlorococcus*, *Gordonia*, and *Sphingomonas* (Table S2). Isolates 50 and 35 carried the highest number of intact prophages, 8 and 7, respectively (Table S2 and Fig. 4A). The P-SSM2-like phage of *Prochlorococcus* found in isolate 50 showed the highest number of proteins similar to those in the region (Table S2), while the ΦC2-like phage in isolate 35 displayed a high number of “hit_genes_count” in bracket (8 out of 9) with ΦC2 (Table S2). The prophages found within the ST 37 and ST 81 isolates were diverse, although ΦCD506 was predominant. No obvious correlation was found between prophage type and STs. Future studies will focus on the role of these elements in the *C. difficile* evolution and infection.

A total of 464 CRISPR arrays, composed of different copies of direct repeat (DR) sequences, and separated by unique spacers were identified in the tested isolates from clade 4 (Table S3). The number in each isolate varied from 5 to 19, and the length ranged from 60 to 1,608 bp (Table S3). In total, 90 of the CRISPR arrays displayed homology with prophages (Table S3). Isolates 10122, 11032, 29, and GZ8 harbored prophages without homologous CRISPR sequences (Table S3).

Sixteen potential plasmid sequences with almost 100% coverage were identified among the 37 isolates (Table S4) and were found to contain important antimicrobial resistance genes (*aadE*, *aad9*, *ermB*, *tetM*, *tetS*, and *tetO*) (Table S4).

Distinctions of PaLoc and CdtLoc regions in clade 4. Three types of toxin gene profiles in clade 4 were covered in this study: A⁺B⁺ (ST332), A⁻B⁺ (ST81 and ST37), and A⁻B⁻ (ST39 and ST109) (Table 1). All isolates in this study were binary toxin negative (Table 1). Based on gene formation, six types of PaLoc were classified in this study (Fig. 5A). Type 1 (ST332) displayed intact gene composition and sequences, while all genes were lost with the exception of 115 bp remaining in type 6 (ST39 and ST109)

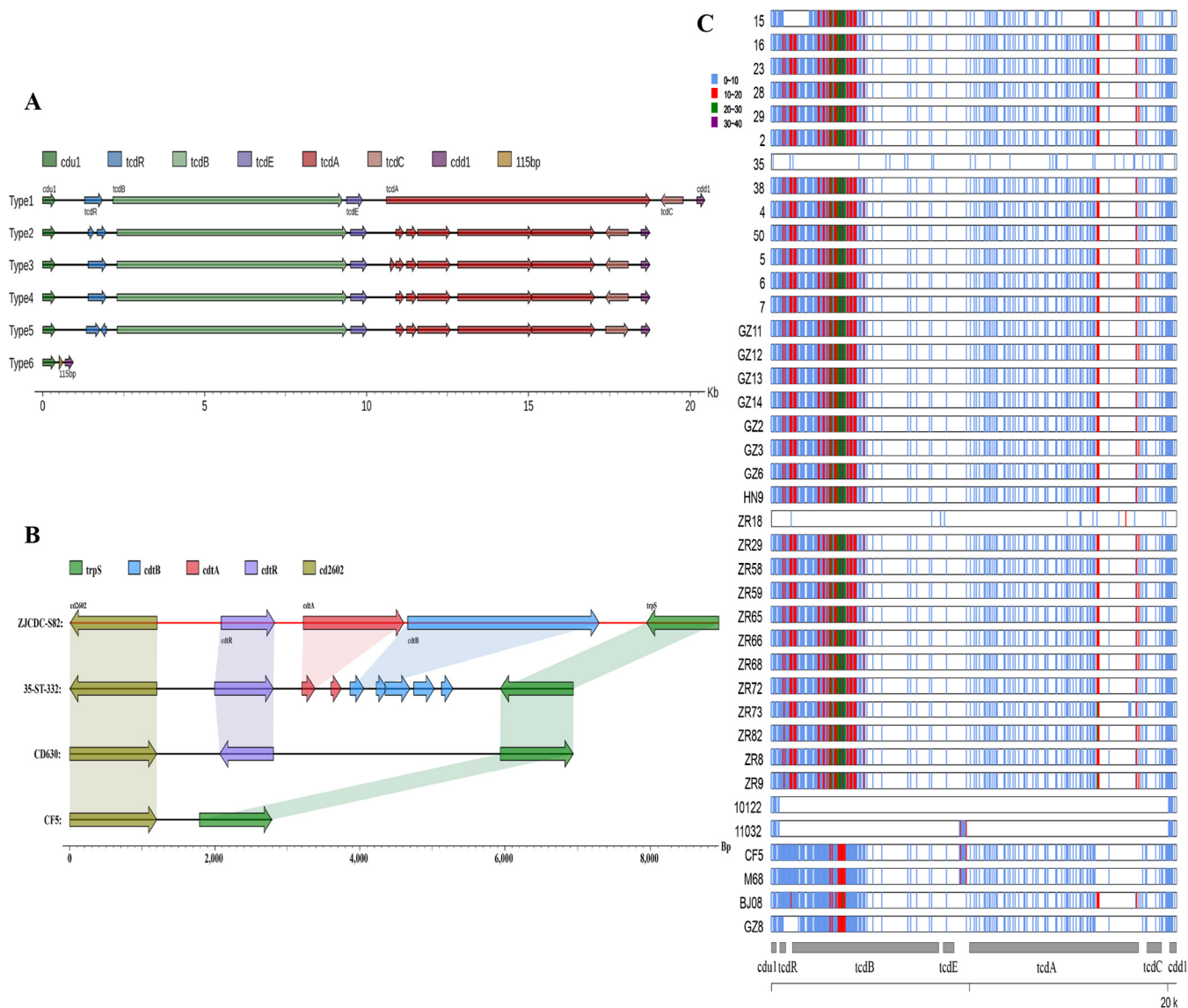


FIG 5 PaLoc and CdtLoc analysis of 37 *C. difficile* isolates from clade 4. (A) Several types were divided based on gene composition of PaLoc. (B) Gene composition of CdtLoc within clade 4. (C) SNPs distributed within PaLoc of all 37 *C. difficile* isolates from clade 4.

(Fig. 5A). The other four types lack a complete and continuing *tcdA* gene, attributed to insertions and single nucleotide polymorphisms (SNPs), which led to termination of *tcdA* gene translation (Fig. 5A). Compared with CD630, the SNPs of genes located within PaLoc regions are shown for each isolate in Fig. 5B. In general, diversity within PaLoc regions correlated with its ST type, with some exceptions (Fig. 5B). For example, isolate 15 within ST81 and ZR18 within ST37 showed distinct SNP distribution (Fig. 5B). The *tcdB* gene demonstrated great heterogeneity, followed by *tcdA*. With the exception of isolate 35, all tested isolates lacked the CdtLoc region (Fig. 5C). Isolate 35 contained a complete *cdtR* gene and fragments of *cdtA* and *cdtB* genes (Fig. 5C).

Antimicrobial resistance gene and related antimicrobial susceptibility. In this study, 60 antibiotic resistance genes were identified by comparison with the ARDB and CARD databases (35, 36). These antibiotic resistance genes belonged to the following antimicrobial classes: fluoroquinolones, β -lactam antibiotics, macrolides, aminocoumarin, rifampin, glycopeptides, tetracycline, macrolide-lincosamide-streptogramin (MLS), chloramphenicol, trimethoprim, streptomycin, aminoglycoside, bacitracin, and lipopeptide (Fig. 6). Most isolates carried approximately 13 to 16 copies of the *macB*

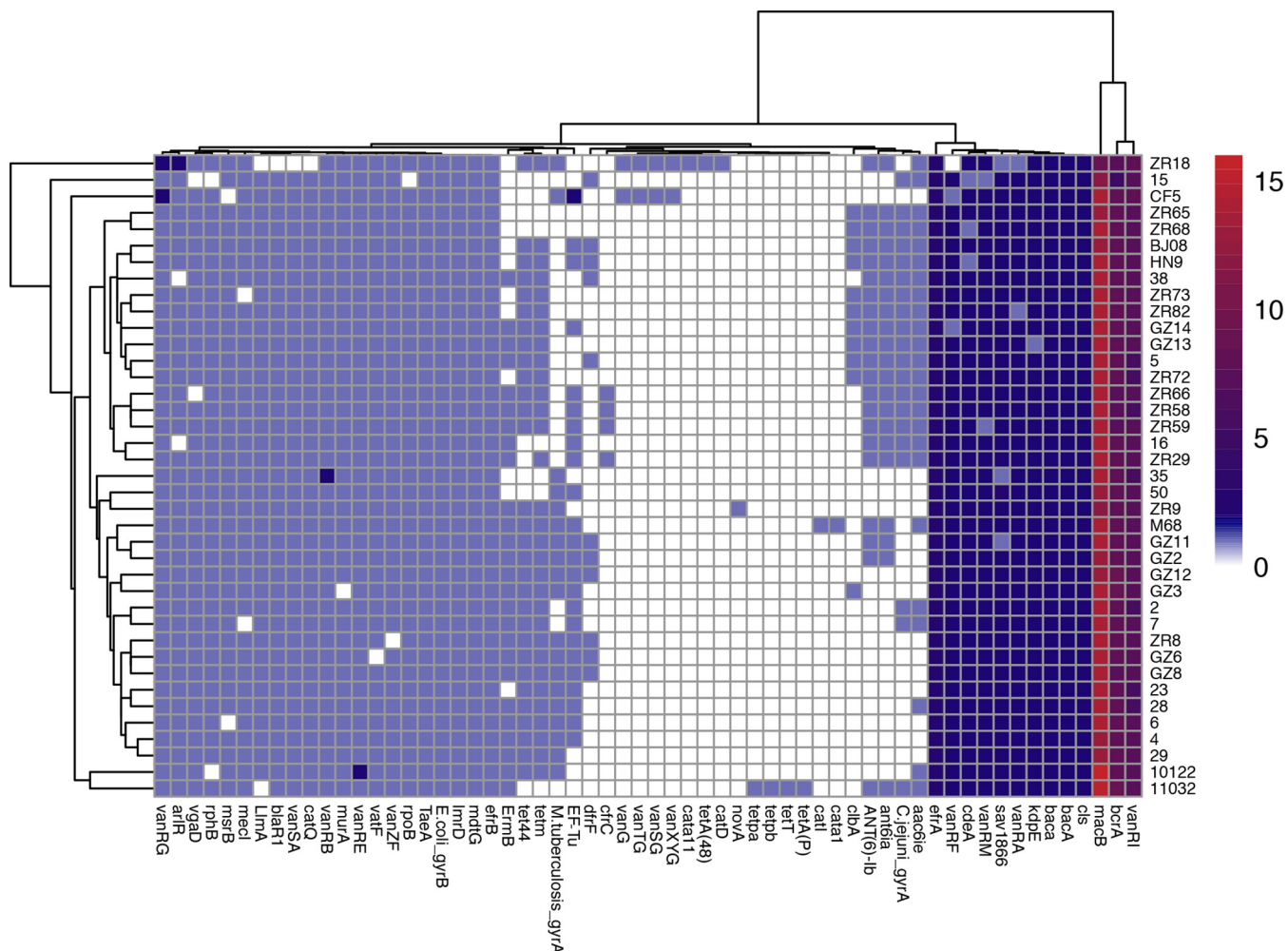


FIG 6 Antibiotic resistance genes of 37 *C. difficile* isolates predicted through comparison with the CARD and ARDB databases. The vertical coordinates refer to 37 *C. difficile* isolates, while the horizontal coordinates refer to the antibiotic-resistant genes identified.

gene, except for ZR18 carrying 9 copies. The next highest numbers of copies were for the *vanRI* and *bcrA* genes (Fig. 6). Remarkably, some isolates carried a unique antibiotic resistance gene cassette, for example, ZR18 and CF5 contained a unique antibiotic resistance gene cluster of approximately 6 kb comprising *vanXYG*, *vanSG*, *vanTG*, and *vanG*, which were integrated as glycopeptide resistance gene (Fig. 6). Additionally, ZR18 also carried *catD* (carried by Tn4453a/b), and *cata11*, which are related to chloramphenicol resistance, and *tetA(48)* (Fig. 6). No functional vancomycin resistance operon was identified here. Furthermore, isolate 11032 contained unique *tetA(P)*, *tetT*, *tetpb*, and *tetpa* genes (Fig. 6). In addition, ZR9 carried a unique *novA* gene, and M68 had unique *cata1* and *catI* genes (Fig. 6).

According to the Etest results, all isolates except for 10122 and 35 were MDR strains, maintaining a resistance rate as high as 97.30%. Details are summarized in Table 2. Almost all MDR strains displayed high levels of drug resistance (Table 2) with quinolone exhibiting 100% resistance to CIF, followed by LVX (97.30%) and MXF (56.76%) (drug abbreviations in “Antimicrobial susceptibility tests” in Materials and Methods) (Table 2). The quinolone resistance is due to a point mutation and substitution within *gyrA* and/or *gyrB*. Clade 4 *C. difficile* retained high-level resistance (91.89%) to ERY compared with the other isolates of other clades reported in Table 2. The *ermB* gene, encoding an antibiotic target-modifying enzyme, is related to MLS resistance. The *ermB* gene was detected in 25 of 34 ERY-resistant isolates (73.53%). ERY resistance is attributed to

TABLE 2 Antimicrobial resistance results and correlation with ST types and antibiotic resistance genes

Drug (concn range [$\mu\text{g/ml}$])	No. of resistant isolates (%) ^a	ST ^b	No. of genes identified ^b	MIC ($\mu\text{g/ml}$) ^b
MXF (0.002–32)	21 (56.76)	ST81 (4), ST109 (1), ST37 (16)	<i>E. coli gyrB</i> (37), <i>M. tuberculosis gyrA</i> (18), <i>C. jejuni gyrA</i> (20)	≥ 32 (21)
LVX (0.002–32)	36 (97.30)	ST332 (1), ST39 (1), ST109 (1), ST81 (4), ST37 (29)	As above	≥ 32 (35) $\geq 8 < 32$ (1)
CIF (0.002–32)	37 (100)	ST332 (1), ST39 (1), ST109 (1), ST81 (4), ST37 (30)	As above	≥ 32 (36) $\geq 8 < 32$ (1)
CLI (0.016–256)	33 (89.19)	ST81 (4), ST109 (1), ST37 (28)	<i>ermB</i> (25), <i>cfrC</i> (4), <i>clbA</i> (11)	≥ 256 (32) $\geq 8 < 256$ (1)
TET (0.016–256)	13 (35.14)	ST81 (2), ST37 (11)	<i>tetA(P)</i> , <i>tetT</i> , <i>tetpb</i> , <i>tetpa</i> were only in isolate 11032; <i>tetA(48)</i> ^c was only in ZR18; <i>tetM</i> (31), <i>tet44</i> (30)	$\geq 16 < 32$ (13)
ERY (0.016–256)	34 (91.89)	ST81 (4), ST39 (1), ST109 (1), ST37 (28)	<i>ermB</i> (25), <i>macB</i> (37), <i>cfrC</i> (4)	≥ 256 (32) $\geq 128 < 256$ (2) $\geq 8 < 128$ (1)
CHL (0.016–256)	11 (29.73)	ST37 (11)	<i>cata11</i> was only in ZR18; <i>cata1</i> was only in M68	≥ 256 (8) $\geq 128 < 256$ (1) $\geq 32 < 128$ (2)
MEM (0.002–32)	19 (51.35)	ST81 (1), ST109 (1), ST37 (17)	<i>blaR1</i> (36), <i>mecl</i> (35)	≥ 32 (15) $\geq 16 < 32$ (4)
RIF (0.002–32)	18 (48.65)	ST37 (18)	<i>rpoB</i> (36), <i>rphB</i> (34)	≥ 32 (18)
VAN (0.016–256)	0	0	<i>vanXYG-vanSG-vanTG-vanG</i> gene cluster was only in ZR18; <i>vanRI</i> (37), <i>vanRM</i> (37), <i>vanRA</i> (37), <i>vanRF</i> (36), <i>vanZF</i> (36), <i>vanRE</i> (37), <i>vanRB</i> (37), <i>vanSA</i> (36), <i>vanRG</i> (37), <i>arlR</i> (34)	≤ 0.5
MET (0.016–256)	0	0	None	≤ 1

^aValues in parentheses show the percentage of isolates resistant to a single drug.

^bValues in parentheses show the number of isolates with the ST, gene, or MIC.

^cGene name.

methylation of position 2058 in 23S rRNA; however, the exact mutation in ERY-resistant *C. difficile* isolates remains to be identified in the future. In addition, high copy numbers of the macrolide resistance *macB* gene, encoding a macrolide ABC transporter protein, were identified in all the tested isolates (Fig. 6). The rate of resistance to CLI was 89.19%, with a high level of resistance detected among the isolates. The rate of resistance to CHL was lower (29.73%) and related to *cata11* and *cata1*, which were identified only in isolates ZR18 and M68, respectively, indicating the existence of other mechanisms of CHL resistance. It is worth mentioning that *catD*, normally carried by *Tn4453a/b* and also responsible for CHL resistance (Fig. 3), was present in isolate ZR18, which showed an intermediate level of CHL resistance (MIC = 64 $\mu\text{g/ml}$). However, *catD* was replaced by another five genes in isolates 7, 2, and 28, which were CHL susceptible. The five new replacement genes included *aac(6')* *aph(2')*, which is correlated significantly with HLGR and is responsible for aminoglycoside resistance, leading to gentamicin and amikacin resistance in isolates 7, 2, and 28. The rates of MEM (51.35%) and RIF (48.65%) resistance were similar among the clade 4 *C. difficile* isolates. All isolates resistant to CHL and RIF were ST37 (Table 2). The *rpoB* and *rphB* genes with several mutations related to RIF

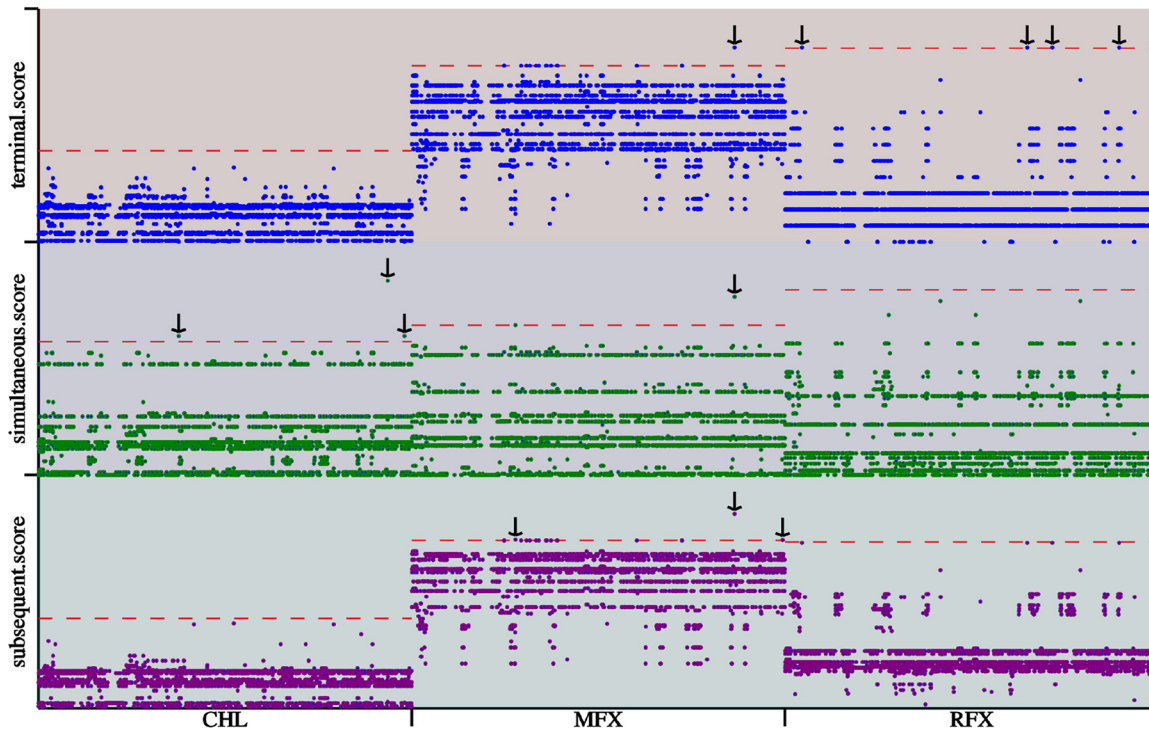


FIG 7 The whole-genome sequence analysis of antimicrobial resistance among 37 *C. difficile* isolates using treeWAS software. The vertical coordinates represent three different calculating methods, which are displayed in three distinct colors. The horizontal coordinates refer to three drugs. The significant SNPs related to each drug are highlighted by black arrows.

resistance were detected in almost all isolates. The mechanism underlying this resistance involves substitution of several nucleotides in the *rpoB* gene. None of the clade 4 isolates were resistant to VAN or MET, although VAN-related genes or gene cassettes were identified.

Genome-wide association analysis of resistance genes. According to our analysis, antimicrobial susceptibility does not correlate well with genotypes. To explore other potential sites responsible for drug resistance, we performed genome-wide association study (GWAS) analysis. Significantly related SNPs were detected in relation to resistance to CHL, MFX, and RIF (Fig. 7). Three significant SNPs associated with CHL resistance were located within an intergenic genetic region (IGS) (Fig. 8), which may play a role in methylation and regulation of cell function. Three remarkable nonsynonymous SNPs associated with MFX resistance (Fig. 7) were detected in genes encoding inosine-uridine-preferring nucleoside hydrolase family protein and the ABC transporter and in the *gyrA* gene, which are reported to be associated with quinolone resistance, and were detected using all three methods (Fig. 7). All MFX-resistant isolates except for GZ11 and 28 displayed the point mutation (Thr→Ile) in *gyrA* compared with susceptible isolates (Fig. 8). In addition, only one MFX-susceptible isolate ZR66 carried the Thr→Ile mutation in *gyrA* (Fig. 8). As shown in Fig. 7, four significant SNPs significantly related to RIF resistance were identified as following: a gene (*dacC* or *dacD*) encoding D-alanyl-D-alanine carboxypeptidase protein, also known as penicillin-binding protein (WP_022616436.1), gene *merR* encoding the transcriptional regulator (WP_022616524.1), a gene involved in replication, recombination, and repair (WP_022616400.1), and a gene in an IGS region (Fig. 8). Most of the RIF-resistant isolates carried the point mutation Ala→Val, Thr→Ile, and Val→Gly in these genes, respectively, with the exception of isolates GZ3, 6, 29, and 23 (Fig. 8). The RIF-susceptible isolates 5 and 38 carried the same mutations (Fig. 8).

DISCUSSION

Due to rapid progress in WGS techniques, the global population structure of *C. difficile* is defined as 5 main clades (clades 1 to 5). ST37 (RT017), which is a well-known

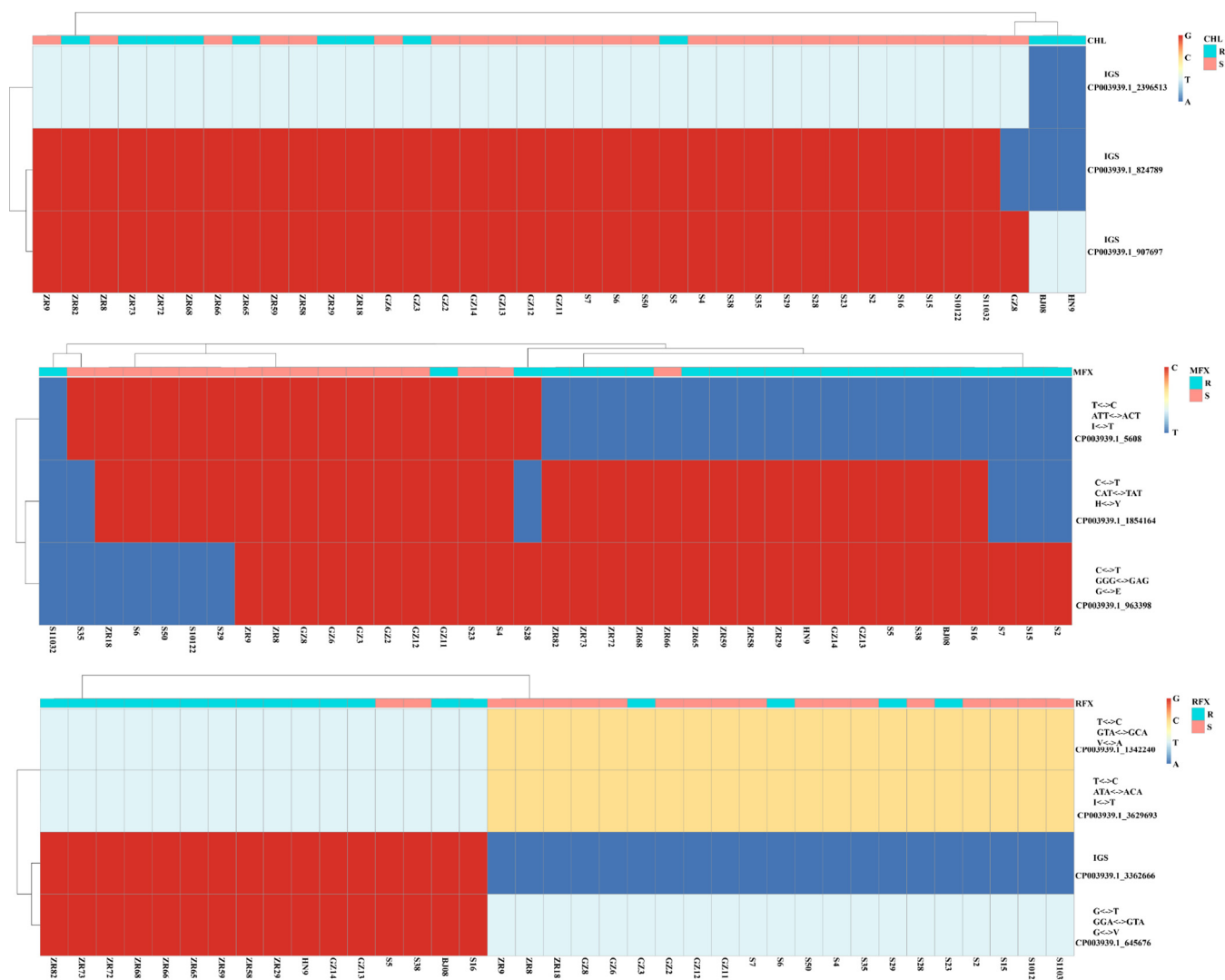


FIG 8 Heatmap of point mutations associated with drug resistance among all 37 *C. difficile* isolates. The drug, nucleotide, codon, amino acid, and gene ID are shown on the right vertical axes. The name of each isolate is shown on the horizontal axes. Nucleotides A, T, C, G are represented by dark blue, light blue, yellow, and red, respectively. R, resistance; S, susceptible.

representative of clade 4, has caused outbreaks in Europe and in the United States, and is documented as the major type associated with CDI in Asia (8). In addition to ST37, clade 4 contained some diversity, such as ST332 (A⁺B⁺), ST39 and ST109 (A⁻B⁻), ST81 (A⁻B⁺), and ST86 (A⁻B⁺). ST332 is a novel type previously identified by our group (37). In this study, we analyzed and compared the whole-genome sequences of 37 clinical *C. difficile* isolates from clade 4. M68 and CF5 were included as isolates of clade 4, and CD630 was used as reference. We further explored the presence of Tn/CTNs, prophages, and CRISPRs and compared their characteristics among the isolates in this clade. The antimicrobial phenotypes of these isolates were determined, and possible antibiotic resistance-related genes were identified. In this study, we aimed to clarify the genetic heterogeneity and microevolution within clade 4 to provide potential explanations for the mechanisms of pathogenesis and antibiotic resistance of *C. difficile*.

The basic features, including GC% and genome size, of the clade 4 isolates from China investigated in this study were similar to those have been reported previously (3). The *C. difficile* genome is highly mosaic and dynamic in structure because of a high proportion of MGEs. CTNs, also known as integrated conjugative elements (ICEs), are capable of excision, transfer, and integration into the chromosome or plasmids, result-

ing in the formation of a circular intermediate (12). Within *C. difficile*, there are two main families of CTNs, known as the Tn916- and the Tn1549-like elements. Tn916 is an 18-kb conjugative transposon that encodes resistance to tetracycline and minocycline via the ribosomal protection protein, Tet (M), and contains 24 potential ORFs. Tn1549, a 34-kb vancomycin resistance element controlled via the *vanB* operon, was originally described in *E. faecalis*. In CD630, six putative CTNs belonging either to the Tn916-like family (CTn1, CTn6, CTn7 plus Tn5397, previously known as CTn3) or to the Tn1549-like family (CTn2, CTn4, and CTn5) were identified. Tn916-like, CTn1-like, and CTn5-like were reported from M68, while CTn5-like was found in CF5. In this study, CTn5-like, Tn5397, and Tn916 elements were identified, with CTn5-like found to exist widely among the investigated clade 4 isolates. However, other transposons, which did not belong to either the Tn916-like or Tn1549-like families, were also discovered, including Tn4453a/b-like, Tn5398-like, and Tn6194-like. Furthermore, two novel putative transposons having regions of homology with CTn2 and CTn7 were identified in isolates ZR9 and ZR18, respectively. It is remarkable that in Tn4453a/b, *catD* was replaced by *aac(6')* *aph(2'')* in isolates 2, 7, and 28, resulting in susceptibility to CHL but resistance to gentamicin and amikacin. The three isolates, which were all ST8, were obtained from elderly hospitalized patients treated with quinolone and carbapenem for 5 days. However, isolate ZR18 carried a typical Tn4453a/b element with *catD*, leading to CHL resistance. The *aac(6')* *aph(2'')* gene, displaying 100% identity and coverage with *C. jejuni*, was first reported in *C. difficile*. This gene encodes a bifunctional AME, accounting for HLG resistance rates in >90% *E. faecalis* and *E. faecium* isolates (38). This illustrated that HGT may occur between *C. difficile* and other intestinal bacteria, leading to unique microevolution of individual isolates. However, the mechanisms by which the local microenvironment causes HGT and the ability of Tn4453a/b containing *aac(6')* *aph(2'')* to transfer between *C. difficile* isolates and/or *C. difficile* and other bacteria remains to be elucidated. Furthermore, two novel transposons with regions with homology to CTn2 and CTn7 were identified. One novel transposon, in isolate ZR9, contained 10 unique genes showing identity with diverse transposons of diverse origins in *C. difficile*, although the remaining 26 genes were homologous with CTn2. The other transposon, in isolate ZR18, lacked 10 out of 24 coding genes present in CTn7. The 10 novel genes also displayed identity with *C. difficile* or other gut pathogens of heterogeneous origins. This situation further suggested that “personalized” HGT occurred in individual isolates, resulting in diversity and genome evolution in *C. difficile*. Great diversity was also exhibited among the other CTNs identified in this study even within the same STs, and several types were classified according to their gene structure and composition.

Sequencing of a number of *C. difficile* genomes has facilitated the identification of numerous putative prophages by bioinformatic analyses, and the role of prophages in its evolution and virulence has become the focus of recent research. So far, only a limited number of temperate phages infecting *C. difficile* have been fully characterized in terms of WGS and morphology by transmission electron microscopy (TEM). Φ CD119, Φ C2, Φ CD27, Φ MMP02, and Φ MMP04 are members of the *Myoviridae* family, while Φ CD38-2 and Φ CD6356 are members of the *Siphoviridae* family. In this study, WGS revealed distribution of various numbers of prophages in all isolates. The top seven main prophages in clade 4 were Φ CDHM19, Φ CD506, Φ MMP01, Φ MMP03, Φ MMP02, Φ MMP04, and Φ C2, all of which belong to the *Myoviridae* family. Some prophages (Φ MMP01, Φ MMP03, Φ MMP02, and Φ MMP04) were induced and isolated from fecal supernatant of CDI patients (34). In addition, Φ C2 mediates transduction of Tn6215, encoding erythromycin resistance, between *C. difficile* isolates (11). Our next step is to induce phages of these isolates and confirm their function experimentally.

The CRISPR-Cas systems, which are present in most archaea and many bacteria, provide adaptive resistance against invasive genetic elements, such as phages and plasmids (40, 41). CRISPR array consists of partial palindromic repeats (DR) interspersed by unique DNA sequences (spacers) that are derived from foreign genetic elements in a linear, time-resolved manner (41, 42). Whole-genome analysis of *C. difficile* strain 630 (ST54/RT012) showed that the CRISPR spacer sequence exhibited similarity to *C. difficile*

phages and plasmids, suggesting CRISPR interference against these mobile elements, which was later experimentally confirmed in the R20291 strain (ST1/RT027/B1) (3, 43). Recently, in a comprehensive analysis of the CRISPR-Cas system in 217 *C. difficile* genomes, a single type IB CRISPR-Cas system and a total of 1,865 CRISPR arrays were identified with *cas* gene clusters present at conserved chromosomal locations (44). The CRISPR arrays of *C. difficile* were markedly enriched (12.5 arrays/genome) in this study compared with other species and previous reports of *C. difficile* (8.5 arrays/genome) (45). Numerous CRISPR arrays (90/464) were homologous to prophages identified among the clade 4 *C. difficile* isolates in this study. CRISPR-Cas has been used for outbreak tracking in *Yersinia pestis* (46) and *Salmonella enterica* subspecies (47), and correlating with important phenotypes, such as antibiotic -resistance cassettes in enterococci (48), and prophages in *Streptococcus pyogenes* genomes (49). All these correlations reflect the role of CRISPR-Cas systems in controlling HGT, as well as the uptake and dissemination of particular genes and operons involved in bacterial adaptation and pathogenesis (50), and hence the evolution of specific species. In our study, we identified another potential method of phylogenetic analysis and genotyping within clade 4 or closely related isolates according to the CRISPR arrays.

Rates of antibiotic resistance vary considerably in different studies, probably depending on the geographic regions and local or national antibiotic policy. In our study, the MDR isolates account for 94.6% of all resistant isolates, which is a much higher proportion than reported previously (55%) in Europe and China (19, 51, 52). Many of the hypervirulent RT027 and RT078 strains are known to exhibit MDR. In a 4-year study in China, MDR isolates with ST37 accounted for the highest proportion (78.2%) of all the tested isolates (53–55). A similar situation was observed in our study, which further illustrates that antibiotic usage promotes independent acquisition of drug resistance, regardless of molecular type.

Resistance to fluoroquinolones has increased dramatically in recent years; for example, the rates of resistance to LVX and CIP reached almost 100% in many studies around the world (51), including our study. Genomic mutations in *gyrA* and/or *gyrB*, known as the quinolone resistance-determining region, QRDR, are involved with resistance to fluoroquinolones (56). The amino acid substitution Thr-82Ile in GyrA was found to be responsible for moxifloxacin resistance (57). Some other substitutions in *gyrA* and/or *gyrB* have been reported in other studies, such as Ser-366Val, Ser-416Ala, Asp-426Asn, and Glu-466Val (58). According to our GWAS analysis, the Thr→Ile mutation in the *gyrA* gene is highly related to MXF resistance in clade 4 *C. difficile* isolates.

RIF resistance was very recently detected, and studies conducted from 2008 to 2010 in different European countries showed variability in the rates of resistance to this antibiotic in *C. difficile* strains, ranging from 6.3% to 36.8% (58). In our study, the rate of RIF resistance reached 48.65%, which is even higher than that reported in a systematic meta-analysis of drug resistance of *C. difficile* infections in mainland China (52). Different SNPs (His-502Asn and Arg-505Lys) within the *rpoB* gene encoding the β -subunit of the RNA polymerase have been identified in RIF-resistant strains (59). Another RIF resistance-related gene, *rphB*, was also detected in 34 isolates in this study but at a low related rate. The existence of some specific substitution in *rphB* that is responsible for RIF remains to be investigated.

In *C. difficile*, resistance to CLI and ERY is common in Europe (55% and 47%, respectively) (19), and in China (70% to 80%) (60), while in our study the rate was more than 90%. In this study, several genes were identified with *ermB*, high copy numbers of *macB*, and *cfrC*, although the correlation between the phenotype and the harbored gene is low. In pan-Europe studies, the rate of TET resistance has been reported to range from 2.4% to 41.67% (51), and the rate in the present study was slightly lower than the highest level at 35.14%. Moreover, the emergence of reduced TET susceptibility increased in our study. In *C. difficile*, TET resistance is commonly conferred by a *tet(M)* carried by a Tn5397 transposon. In our study, 29 isolates contained Tn5397; however, *tetM* was absent from isolates ZR73 and 5. Among these 27 isolates, the rate of TET resistance was 40.74% (11/27). For eight isolates without Tn5397, two resistant

isolates (15 and 16) and one intermediate strain (11032) were still identified. In addition, no other TET resistance-determining genes, including *tet 44* and *tetW* (other important genes responsible for TET resistance in *C. difficile* especially with animal and environmental origins) were detected in these three isolates. This indicates the possible existence of another mechanism of TET resistance.

Although CHL resistance is not so common in Europe (3.5%) and China (2%) (19, 52), the rate obviously increased in our study (29.73%). It is known that *catD* in Tn4453a/b mediates CHL resistance; however, in our study, only one (ZR18) of 11 resistant isolates carried *catD* in Tn4453a/b and *cata11* in the genome, which may represent another mechanism of gaining CHL resistance in *C. difficile*. The great heterogeneity in the genetic arrangement of those resistance determinants confirms that genetic exchange and recombination frequently occur in individual clinical strains.

As reported in a previous study in China, no resistant isolates to MTZ and VAN or isolates with reduced MTZ susceptibility were found here, although reduced MTZ susceptibility was occasionally reported in Europe (61). The mechanism of MTZ resistance is still not completely understood. Nitroimidazole (*nim*) genes conferring resistance to MTZ in *Helicobacter pylori* have not been identified in *C. difficile*. The defined mechanism of resistance is a multifactorial process involving alterations in different metabolic pathways, such as nitroreductase activity, iron uptake, and DNA repair (59). A *vanB* operon originally described in *E. faecalis* harboring Tn1549 is responsible for resistance to VAN (62). Although several Tn1549-like elements have been reported in *C. difficile*, no functional *vanB* operon was identified. Recently, a *vanG*-like gene cluster, homologous to the cluster found in *E. faecalis*, has been reported in a number of *C. difficile* isolates. However, although this cluster is expressed, it does not promote resistance to VAN (63). The same situation was found in isolate ZR18 in our study with a series of *vanG*-like gene clusters identified, without resistance to VAN.

In conclusion, we analyzed HGT-related elements involved in shaping the genome and biological features, including antibiotic susceptibility phenotype of *C. difficile* from clade 4 with varied STs isolated in China. Our findings provide important new insights into the mechanism of genome remodeling within clade 4 and offer a new method for typing and tracing the origins of closely related isolates.

MATERIALS AND METHODS

Isolates and preparation of genomic DNA. A total of 37 clinical *C. difficile* isolates from clade 4 with divergent origins in China were included in this study (Table 1). These isolates comprised five ST types: one ST332 isolate (a new type identified in our previous study), four ST 81 (RT 017), one each of ST 39 (RT 085) and ST109, and 30 ST 37 (RT 017) isolates. Details of these isolates are summarized in Table 1. Strains CD630 (GenBank accession no. AM180355), CF5 (FN665652), and M68 (FN668375) were used as references throughout the investigation.

All 37 isolates were cultured on brain heart infusion (BHI) agar plates (Oxoid, Basingstoke, UK) supplemented with 5% sheep blood (BaoTe, Beijing, China) in an anaerobic environment (80% nitrogen, 10% hydrogen, and 10% carbon dioxide) (Mart, NL) at 37°C for 48 h. Typical colonies were picked and recultured on BHI for 24 h before preparation of genomic DNA using the Wizard Genomic DNA purification kit (Promega, Madison, WI, USA) according to the manufacturer's instructions.

MLST, PCR ribotyping, and toxin gene profiling. The MLST, PCR ribotyping, and toxin gene profiling information was obtained according to previously reported methods (37, 64).

Whole-genome sequencing and assembly. Whole-genome sequencing (WGS) was performed on the Illumina PE150 (Illumina Inc., USA) with average insert lengths of 350 bp. Raw data were processed in four steps: removal of reads with 5 bp of ambiguous base, reads with 20 bp of low quality (\leq Q20), adapter contamination, and duplicated reads. Finally, filtered reads were assembled using SOAP denovo v2.04 (65, 66).

Genome annotation and phylogenetic analysis. Genes were predicted using GeneMarkS version 3.05 (67) and aligned with databases to obtain the annotation corresponding to their homologs, with the highest quality alignment result chosen as the gene annotation. Gene functions were predicted by whole-genome BLAST (<http://blast.ncbi.nlm.nih.gov/Blast.cgi>) searches against the following databases: Gene Ontology (GO) (68), Kyoto Encyclopedia of Genes and Genomes (KEGG) (69), Clusters of Orthologous Groups (COG) (70), Non-Redundant Protein (NR) databases (71), Transporter Classification Database (TCDB) (72), and Swiss-Prot (73). tRNA genes were predicted by tRNA scan-SE (74). rRNA genes were analyzed by rRNAmmer (75). Small nuclear RNAs (snRNA) were predicted by BLAST searches against the Rfam (76) database.

Single core genes were obtained from the clustering results of all sample genes used by CD-HIT version 4.6. A phylogenetic tree was built using the neighbor-joining method based on 2,456 single core genes using MEGA6.0 with 1,000 replicates (77).

Analysis of MGEs. All the transposons (Tns) and conjugative transposons (CTns) were identified using BLAST searches of the *C. difficile* genome sequences or transposon sequences available at NCBI (<https://www.ncbi.nlm.nih.gov/>) with identity and coverage requirements set at >80%. Prophages were identified using the PHASTER web server (<http://phast.wishartlab.com>). The intact, questionable, and incomplete prophage sequences were defined by score values of >90, 70 to 90, and <70, respectively (78). To identify plasmids, reads were assembled into contigs using the SOAP denovo. Contigs were then screened for plasmids using Microbial Genome BLAST searches against the NCBI complete plasmid database (<ftp://ftp.ncbi.nlm.nih.gov/genomes/refseq/plasmid/>). The potential plasmids were defined as $\geq 70\%$ coverage and $\geq 80\%$ identity. The CRISPRFinder (79) was used for CRISPR identification.

Sequence analysis of PaLoc and CdtLoc. The PaLoc and CdtLoc were confirmed by comparison with the reference CD630 genome. Orthologous genes were detected by BLAST (version 2.2.12) searches with >80% coverage and >90% nucleotide identity. The genetic structure as well as insertions and deletions (indels) were studied.

Antimicrobial susceptibility tests. *C. difficile* isolates were tested for susceptibility to moxifloxacin (MXF), vancomycin (VAN), clindamycin (CLI), tetracycline (TET), erythromycin (ERY), rifampin (RIF), levofloxacin (LVX), chloramphenicol (CHL), metronidazole (MTZ), ciprofloxacin (CIP), and meropenem (MEM) using Etest strips (bioMérieux, France, and Liofilchem, Italy). Tests to gentamicin (CEN) and amikacin (AMK) were also performed with isolates 2, 7, 28, and ZR18 using Etest strips (bioMérieux, France, and Liofilchem, Italy). The MICs for MTZ, MXF, CLI, CIP, LVX, and TET were determined according to recommendations of the Clinical and Laboratory Standards Institute (CLSI) M11-A7 and M100-S24 (80, 81), and the European Committee on Antimicrobial Susceptibility Testing (EUCAST) (<http://www.eucast.org>). The breakpoints for VAN, RIF, ERY, CHL, and meropenem were determined according to a previous study (54, 58). Multidrug resistance (MDR) was defined as resistance to at least three antimicrobial classes. *C. difficile* ATCC 700057 was included as a control in each experiment (82).

Antimicrobial resistance genes were predicted through comparison with the Antibiotic Resistance Genes Database, ARDB (<https://ardb.cbc.umd.edu/>) (35), and the Comprehensive Antibiotic Resistance Database, CARD (<https://card.mcmaster.ca/>) (36). Heatmap analysis was performed using the pheatmap package, and statistics packages in R software (version 2.15.3).

Single nucleotide polymorphisms detected and association analysis. Single nucleotide polymorphisms (SNPs) were detected by comparing the sequence of each isolate with that of strain BJ08. SNP calling was detected using the NUCmer program in the MUMer package (V3.23). All primary SNPs were further evaluated in contigs to validate alleles. Sequence regions of 201 bp, which included 100 bp extracted from either side of the referenced SNP site, were subjected to BLAST analysis with sample contigs. The SNPs were removed if the alignment length was less than 101 bp. In addition, the SNPs located in repeat regions predicted by RepeatMasker (version open-4.05) and TRF (Tandem Repeats Finder; version 4.07b) of the reference were also excluded. Genome-wide association studies (GWAS) were conducted using the open-source R package treeWAS, which is freely available at <https://github.com/caitcollins/treeWAS> (83). Three methods (terminal, simultaneous, and subsequent tests) were used to confirm the results in this study.

Data availability. The sequence information from this whole-genome shotgun project of 37 *C. difficile* isolates has been submitted to DDBJ/EMBL/GenBank under the following BioProject accession number [PRJNA479396](https://www.ncbi.nlm.nih.gov/bioproject/PRJNA479396).

SUPPLEMENTAL MATERIAL

Supplemental material for this article may be found at <https://doi.org/10.1128/mSystems.00252-18>.

TABLE S1, PDF file, 0.1 MB.

TABLE S2, XLSX file, 0.1 MB.

TABLE S3, XLSX file, 0.04 MB.

TABLE S4, PDF file, 0.1 MB.

ACKNOWLEDGMENTS

This research was supported by the National Sci-Tech Key Project (grant 2018ZX10733402).

We thank Lei Zhao from Iowa State University for critically reviewing the manuscript.

REFERENCES

1. He M, Miyajima F, Roberts P, Ellison L, Pickard DJ, Martin MJ, Connor TR, Harris SR, Fairley D, Bamford KB, D'Arc S, Brazier J, Brown D, Coia JE, Douce G, Gerding D, Kim HJ, Koh TH, Kato H, Senoh M, Louie T, Michell S, Butt E, Peacock SJ, Brown NM, Riley T, Songer G, Wilcox M, Pirmohamed M, Kuijper E, Hawkey P, Wren BW, Dougan G, Parkhill J, Lawley TD. 2013. Emergence and global spread of epidemic healthcare-associated *Clostridium difficile*. *Nat Genet* 45:109–113. <https://doi.org/10.1038/ng.2478>.
2. Warriner K, Xu C, Habash M, Sultan S, Weese SJ. 2017. Dissemination of *Clostridium difficile* in food and the environment: significant sources of *C. difficile* community-acquired infection? *J Appl Microbiol* 122:542–553. <https://doi.org/10.1111/jam.13338>.

3. Sebaihia M, Wren BW, Mullany P, Fairweather NF, Minton N, Stabler R, Thomson NR, Roberts AP, Cerdeno-Tarraga AM, Wang H, Holden MT, Wright A, Churcher C, Quail MA, Baker S, Bason N, Brooks K, Chillingworth T, Cronin A, Davis P, Dowd L, Fraser A, Feltwell T, Hance Z, Holroyd S, Jagels K, Moule S, Mungall K, Price C, Rabinowitsch E, Sharp S, Simmonds M, Stevens K, Unwin L, Whithead S, Dupuy B, Dougan G, Barrell B, Parkhill J. 2006. The multidrug-resistant human pathogen *Clostridium difficile* has a highly mobile, mosaic genome. *Nat Genet* 38:779–786. <https://doi.org/10.1038/ng1830>.
4. Monot M, Boursaux-Eude C, Thibonnier M, Vallenet D, Moszer I, Medigue C, Martin-Verstraete I, Dupuy B. 2011. Reannotation of the genome sequence of *Clostridium difficile* strain 630. *J Med Microbiol* 60: 1193–1199. <https://doi.org/10.1099/jmm.0.030452-0>.
5. Brouwer MS, Allan E, Mullany P, Roberts AP. 2012. Draft genome sequence of the nontoxigenic *Clostridium difficile* strain CD37. *J Bacteriol* 194:2125–2126. <https://doi.org/10.1128/JB.00122-12>.
6. Stabler RA, He M, Dawson L, Martin M, Valiente E, Corton C, Lawley TD, Sebaihia M, Quail MA, Rose G, Gerding DN, Gibert M, Popoff MR, Parkhill J, Dougan G, Wren BW. 2009. Comparative genome and phenotypic analysis of *Clostridium difficile* 027 strains provides insight into the evolution of a hypervirulent bacterium. *Genome Biol* 10:R102. <https://doi.org/10.1186/gb-2009-10-9-r102>.
7. He M, Sebaihia M, Lawley TD, Stabler RA, Dawson LF, Martin MJ, Holt KE, Seth-Smith HM, Quail MA, Rance R, Brooks K, Churcher C, Harris D, Bentley SD, Burrows C, Clark L, Corton C, Murray V, Rose G, Thurston S, van Tonder A, Walker D, Wren BW, Dougan G, Parkhill J. 2010. Evolutionary dynamics of *Clostridium difficile* over short and long time scales. *Proc Natl Acad Sci U S A* 107:7527–7532. <https://doi.org/10.1073/pnas.0914322107>.
8. Knight DR, Elliott B, Chang BJ, Perkins TT, Riley TV. 2015. Diversity and evolution in the genome of *Clostridium difficile*. *Clin Microbiol Rev* 28:721–741. <https://doi.org/10.1128/CMR.00127-14>.
9. Didelot X, Eyre DW, Cule M, Ip CL, Ansari MA, Griffiths D, Vaughan A, O'Connor L, Golubchik T, Batty EM, Piazza P, Wilson DJ, Bowden R, Donnelly PJ, Dingle KE, Wilcox M, Walker AS, Crook DW, Peto TE, Harding RM. 2012. Microevolutionary analysis of *Clostridium difficile* genomes to investigate transmission. *Genome Biol* 13:R118. <https://doi.org/10.1186/gb-2012-13-12-r118>.
10. Mullany P, Allan E, Roberts AP. 2015. Mobile genetic elements in *Clostridium difficile* and their role in genome function. *Res Microbiol* 166: 361–367. <https://doi.org/10.1016/j.resmic.2014.12.005>.
11. Goh S, Hussain H, Chang BJ, Emmett W, Riley TV, Mullany P. 2013. Phage phiC2 mediates transduction of Tn6215, encoding erythromycin resistance, between *Clostridium difficile* strains. *mBio* 4:e00840-13. <https://doi.org/10.1128/mBio.00840-13>.
12. Brouwer MS, Warburton PJ, Roberts AP, Mullany P, Allan E. 2011. Genetic organisation, mobility and predicted functions of genes on integrated, mobile genetic elements in sequenced strains of *Clostridium difficile*. *PLoS One* 6:e23014. <https://doi.org/10.1371/journal.pone.0023014>.
13. Wasels F, Monot M, Spigaglia P, Barbanti F, Ma L, Bouchier C, Dupuy B, Mastrantonio P. 2014. Inter- and intraspecies transfer of a *Clostridium difficile* conjugative transposon conferring resistance to MLSB. *Microb Drug Resist* 20:555–560. <https://doi.org/10.1089/mdr.2014.0015>.
14. Griffiths D, Lawley W, Kachrimanidou M, Bowden R, Crook DW, Fung R, Golubchik T, Harding RM, Jeffery KJ, Jolley KA, Kirton R, Peto TE, Rees G, Stoesser N, Vaughan A, Walker AS, Young BC, Wilcox M, Dingle KE. 2010. Multilocus sequence typing of *Clostridium difficile*. *J Clin Microbiol* 48:770–778. <https://doi.org/10.1128/JCM.01796-09>.
15. Eyre DW, Cule ML, Wilson DJ, Griffiths D, Vaughan A, O'Connor L, Ip CL, Golubchik T, Batty EM, Finney JM, Wyllie DH, Didelot X, Piazza P, Bowden R, Dingle KE, Harding RM, Crook DW, Wilcox MH, Peto TEA, Walker AS. 2013. Diverse sources of *C. difficile* infection identified on whole-genome sequencing. *N Engl J Med* 369:1195–1205. <https://doi.org/10.1056/NEJMoa1216064>.
16. Stabler RA, Dawson LF, Valiente E, Cairns MD, Martin MJ, Donahue EH, Riley TV, Songer JG, Kuijper EJ, Dingle KE, Wren BW. 2012. Macro and micro diversity of *Clostridium difficile* isolates from diverse sources and geographical locations. *PLoS One* 7:e31559. <https://doi.org/10.1371/journal.pone.0031559>.
17. Janezic S, Rupnik M. 2015. Genomic diversity of *Clostridium difficile* strains. *Res Microbiol* 166:353–360. <https://doi.org/10.1016/j.resmic.2015.02.002>.
18. Bauer MP, Notermans DW, van Benthem BH, Brazier JS, Wilcox MH, Rupnik M, Monnet DL, van Dissel JT, Kuijper EJ. 2011. *Clostridium difficile* infection in Europe: a hospital-based survey. *Lancet* 377:63–73. [https://doi.org/10.1016/S0140-6736\(10\)61266-4](https://doi.org/10.1016/S0140-6736(10)61266-4).
19. Freeman J, Vernon J, Morris K, Nicholson S, Todhunter S, Longshaw C, Wilcox MH, Pan-European Longitudinal Surveillance of Antibiotic Resistance among Prevalent *Clostridium difficile* Ribotypes' Study Group. 2015. Pan-European longitudinal surveillance of antibiotic resistance among prevalent *Clostridium difficile* ribotypes. *Clin Microbiol Infect* 21:248.e9–248.e16. <https://doi.org/10.1016/j.cmi.2014.09.017>.
20. Lim SK, Stuart RL, Mackin KE, Carter GP, Kotsanas D, Francis MJ, Easton M, Dimovski K, Elliott B, Riley TV, Hogg G, Paul E, Korman TM, Seemann T, Stinear TP, Lyras D, Jenkin GA. 2014. Emergence of a ribotype 244 strain of *Clostridium difficile* associated with severe disease and related to the epidemic ribotype 027 strain. *Clin Infect Dis* 58:1723–1730. <https://doi.org/10.1093/cid/ciu203>.
21. O'Connor JR, Johnson S, Gerding DN. 2009. *Clostridium difficile* infection caused by the epidemic BI/NAP1/027 strain. *Gastroenterology* 136: 1913–1924. <https://doi.org/10.1053/j.gastro.2009.02.073>.
22. Tickler IA, Goering RV, Whitmore JD, Lynn AN, Persing DH, Tenover FC. 2014. Strain types and antimicrobial resistance patterns of *Clostridium difficile* isolates from the United States, 2011 to 2013. *Antimicrob Agents Chemother* 58:4214–4218. <https://doi.org/10.1128/AAC.02775-13>.
23. Kuijper EJ, Barbut F, Brazier JS, Kleinkauf N, Eckmanns T, Lambert ML, Drudy D, Fitzpatrick F, Wiuff C, Brown DJ, Coia JE, Pituch H, Reichert P, Even J, Mossong J, Widmer AF, Olsen KE, Allerberger F, Notermans DW, Delmee M, Coignard B, Wilcox M, Patel B, Frei R, Nagy E, Bouza E, Marin M, Akerlund T, Virolainen-Julkunen A, Lytikainen O, Kotila S, Ingebretsen A, Smyth B, Rooney P, Poxton IR, Monnet DL. 2008. Update of *Clostridium difficile* infection due to PCR ribotype 027 in Europe, 2008. *Euro Surveill* 13(31):pii=18942. <https://doi.org/10.2807/ese.13.31.18942-3en>.
24. Chen R, Feng Y, Wang X, Yang J, Zhang X, Lu X, Zong Z. 2017. Whole genome sequences of three Clade 3 *Clostridium difficile* strains carrying binary toxin genes in China. *Sci Rep* 7:43555. <https://doi.org/10.1038/srep43555>.
25. Kuijper EJ, de Weerd J, Kato H, Kato N, van Dam AP, van der Vorm ER, Weel J, van Rheeën C, Dankert J. 2001. Nosocomial outbreak of *Clostridium difficile*-associated diarrhoea due to a clindamycin-resistant enterotoxin A-negative strain. *Eur J Clin Microbiol Infect Dis* 20:528–534.
26. Drudy D, Harnedy N, Fanning S, Hannan M, Kyne L. 2007. Emergence and control of fluoroquinolone-resistant, toxin A-negative, toxin B-positive *Clostridium difficile*. *Infect Control Hosp Epidemiol* 28:932–940. <https://doi.org/10.1086/519181>.
27. Alfa MJ, Kabani A, Lysterly D, Moncrief S, Neville LM, Al-Barrak A, Harding GK, Dyck B, Olekson K, Embil JM. 2000. Characterization of a toxin A-negative, toxin B-positive strain of *Clostridium difficile* responsible for a nosocomial outbreak of *Clostridium difficile*-associated diarrhea. *J Clin Microbiol* 38:2706–2714.
28. Collins DA, Hawkey PM, Riley TV. 2013. Epidemiology of *Clostridium difficile* infection in Asia. *Antimicrob Resist Infect Control* 2:21. <https://doi.org/10.1186/2047-2994-2-21>.
29. Knight DR, Thean S, Putsathit P, Fenwick S, Riley TV. 2013. Cross-sectional study reveals high prevalence of *Clostridium difficile* non-PCR ribotype 078 strains in Australian veal calves at slaughter. *Appl Environ Microbiol* 79:2630–2635. <https://doi.org/10.1128/AEM.03951-12>.
30. Suo J, Yan Z, Wu Y, Li WG, Zhang WZ, Liu XS, Liu Y, Lu J. 2017. *Clostridium difficile* RT 078/ST11: a threat to community population and pigs identified in elder hospitalized patients in Beijing, China. *Infect Control Hosp Epidemiol* 38:1383–1385. <https://doi.org/10.1017/ice.2017.206>.
31. Hallgren A, Saedi B, Nilsson M, Monstein HJ, Isaksson B, Hanberger H, Nilsson LE. 2003. Genetic relatedness among *Enterococcus faecalis* with transposon-mediated high-level gentamicin resistance in Swedish intensive care units. *J Antimicrob Chemother* 52:162–167. <https://doi.org/10.1093/jac/dkg315>.
32. Donabedian SM, Thal LA, Hershberger E, Perri MB, Chow JW, Bartlett P, Jones R, Joyce K, Rossiter S, Gay K, Johnson J, Mackinson C, Debes E, Madden J, Angulo F, Zervos MJ. 2003. Molecular characterization of gentamicin-resistant *Enterococci* in the United States: evidence of spread from animals to humans through food. *J Clin Microbiol* 41: 1109–1113. <https://doi.org/10.1128/JCM.41.3.1109-1113.2003>.
33. Roberts AP, Allan E, Mullany P. 2014. The impact of horizontal gene transfer on the biology of *Clostridium difficile*. *Adv Microb Physiol* 65:63–82. <https://doi.org/10.1016/bs.ampbs.2014.08.002>.
34. Meessen-Pinard M, Sekulovic O, Fortier LC. 2012. Evidence of in vivo

- prophage induction during *Clostridium difficile* infection. *Appl Environ Microbiol* 78:7662–7670. <https://doi.org/10.1128/AEM.02275-12>.
35. Liu B, Pop M. 2009. ARDB—Antibiotic Resistance Genes Database. *Nucleic Acids Res* 37:D443–D447. <https://doi.org/10.1093/nar/gkn656>.
 36. McArthur AG, Waglechner N, Nizam F, Yan A, Azad MA, Baylay AJ, Bhullar K, Canova MJ, De Pascale G, Ejim L, Kalan L, King AM, Koteva K, Morar M, Mulvey MR, O'Brien JS, Pawlowski AC, Piddock LJ, Spanogiannopoulos P, Sutherland AD, Tang I, Taylor PL, Thaker M, Wang W, Yan M, Yu T, Wright GD. 2013. The comprehensive antibiotic resistance database. *Antimicrob Agents Chemother* 57:3348–3357. <https://doi.org/10.1128/AAC.00419-13>.
 37. Liu XS, Li WG, Zhang WZ, Wu Y, Lu JX. 2018. Molecular characterization of *Clostridium difficile* isolates in China from 2010 to 2015. *Front Microbiol* 9:845. <https://doi.org/10.3389/fmicb.2018.00845>.
 38. Kao SJ, You I, Clewell DB, Donabedian SM, Zervos MJ, Petrin J, Shaw KJ, Chow JW. 2000. Detection of the high-level aminoglycoside resistance gene *aph(2'')-Ib* in *Enterococcus faecium*. *Antimicrob Agents Chemother* 44:2876–2879. <https://doi.org/10.1128/AAC.44.10.2876-2879.2000>.
 39. Reference deleted.
 40. Stern A, Mick E, Tirosh I, Sagy O, Sorek R. 2012. CRISPR targeting reveals a reservoir of common phages associated with the human gut microbiome. *Genome Res* 22:1985–1994. <https://doi.org/10.1101/gr.138297.112>.
 41. Makarova KS, Haft DH, Barrangou R, Brouns SJ, Charpentier E, Horvath P, Moineau S, Mojica FJ, Wolf YI, Yakunin AF, van der Oost J, Koonin EV. 2011. Evolution and classification of the CRISPR-Cas systems. *Nat Rev Microbiol* 9:467–477. <https://doi.org/10.1038/nrmicro2577>.
 42. Makarova KS, Wolf YI, Alkhnbashi OS, Costa F, Shah SA, Saunders SJ, Barrangou R, Brouns SJ, Charpentier E, Haft DH, Horvath P, Moineau S, Mojica FJ, Terns RM, Terns MP, White MF, Yakunin AF, Garrett RA, van der Oost J, Backofen R, Koonin EV. 2015. An updated evolutionary classification of CRISPR-Cas systems. *Nat Rev Microbiol* 13:722–736. <https://doi.org/10.1038/nrmicro3569>.
 43. Boudry P, Semenova E, Monot M, Datsenko KA, Lopatina A, Sekulovic O, Ospina-Bedoya M, Fortier LC, Severinov K, Dupuy B, Soutourina O. 2015. Function of the CRISPR-Cas system of the human pathogen *Clostridium difficile*. *mBio* 6:e01112-15. <https://doi.org/10.1128/mBio.01112-15>.
 44. Andersen JM, Shoup M, Robinson C, Britton R, Olsen KE, Barrangou R. 2016. CRISPR diversity and microevolution in *Clostridium difficile*. *Genome Biol Evol* 8:2841–2855. <https://doi.org/10.1093/gbe/evw203>.
 45. Grissa I, Vergnaud G, Pourcel C. 2007. The CRISPRdb database and tools to display CRISPRs and to generate dictionaries of spacers and repeats. *BMC Bioinformatics* 8:172. <https://doi.org/10.1186/1471-2105-8-172>.
 46. Barros MP, Franca CT, Lins RH, Santos MD, Silva EJ, Oliveira MB, Silveira-Filho VM, Rezende AM, Balbino VQ, Leal-Balbino TC. 2014. Dynamics of CRISPR loci in microevolutionary process of *Yersinia pestis* strains. *PLoS One* 9:e108353. <https://doi.org/10.1371/journal.pone.0108353>.
 47. Pettengill JB, Timme RE, Barrangou R, Toro M, Allard MW, Strain E, Musser SM, Brown EW. 2014. The evolutionary history and diagnostic utility of the CRISPR-Cas system within *Salmonella enterica* ssp. *enterica*. *PeerJ* 2:e340. <https://doi.org/10.7717/peerj.340>.
 48. Palmer KL, Gilmore MS. 2010. Multidrug-resistant enterococci lack CRISPR-cas. *mBio* 1:e00227-10. <https://doi.org/10.1128/mBio.00227-10>.
 49. Nozawa T, Furukawa N, Aikawa C, Watanabe T, Haobam B, Kurokawa K, Maruyama F, Nakagawa I. 2011. CRISPR inhibition of prophage acquisition in *Streptococcus pyogenes*. *PLoS One* 6:e19543. <https://doi.org/10.1371/journal.pone.0019543>.
 50. Louwen R, Staals RH, Endtz HP, van Baarlen P, van der Oost J. 2014. The role of CRISPR-Cas systems in virulence of pathogenic bacteria. *Microbiol Mol Biol Rev* 78:74–88. <https://doi.org/10.1128/MMBR.00039-13>.
 51. Freeman J, Vernon J, Pilling S, Morris K, Nicholson S, Shearman S, Longshaw C, Wilcox MH. 2018. The CloSER study: results from a three-year pan-European longitudinal surveillance of antibiotic resistance among prevalent *Clostridium difficile* ribotypes, 2011–2014. *Clin Microbiol Infect* 24:724–731. <https://doi.org/10.1016/j.cmi.2017.10.008>.
 52. Tang C, Cui L, Xu Y, Xie L, Sun P, Liu C, Xia W, Liu G. 2016. The incidence and drug resistance of *Clostridium difficile* infection in Mainland China: a systematic review and meta-analysis. *Sci Rep* 6:37865. <https://doi.org/10.1038/srep37865>.
 53. Cheng JW, Xiao M, Kudinha T, Kong F, Xu ZP, Sun LY, Zhang L, Fan X, Xie XL, Xu YC. 2016. Molecular epidemiology and antimicrobial susceptibility of *Clostridium difficile* isolates from a university teaching hospital in China. *Front Microbiol* 7:1621. <https://doi.org/10.3389/fmicb.2016.01621>.
 54. Jin D, Luo Y, Huang C, Cai J, Ye J, Zheng Y, Wang L, Zhao P, Liu A, Fang W, Wang X, Xia S, Jiang J, Tang YW. 2017. Molecular epidemiology of *Clostridium difficile* infection in hospitalized patients in eastern China. *J Clin Microbiol* 55:801–810. <https://doi.org/10.1128/JCM.01898-16>.
 55. Chen YB, Gu SL, Shen P, Lv T, Fang YH, Tang LL, Li LJ. 2018. Molecular epidemiology and antimicrobial susceptibility of *Clostridium difficile* isolated from hospitals during a 4-year period in China. *J Med Microbiol* 67:52–59. <https://doi.org/10.1099/jmm.0.000646>.
 56. Peng Z, Jin D, Kim HB, Stratton CW, Wu B, Tang YW, Sun X. 2017. Update on antimicrobial resistance in *Clostridium difficile*: resistance mechanisms and antimicrobial susceptibility testing. *J Clin Microbiol* 55:1998–2008. <https://doi.org/10.1128/JCM.02250-16>.
 57. Dridi L, Tankovic J, Burghoffer B, Barbut F, Petit JC. 2002. *gyrA* and *gyrB* mutations are implicated in cross-resistance to ciprofloxacin and moxifloxacin in *Clostridium difficile*. *Antimicrob Agents Chemother* 46:3418–3421. <https://doi.org/10.1128/AAC.46.11.3418-3421.2002>.
 58. Spigaglia P, Barbanti F, Mastrantonio P. 2011. Multidrug resistance in European *Clostridium difficile* clinical isolates. *J Antimicrob Chemother* 66:2227–2234. <https://doi.org/10.1093/jac/dkr292>.
 59. Caspers P, Locher HH, Pfaff P, Diggelmann S, Ruedei G, Bur D, Ritz D. 2017. Different resistance mechanisms for cadazolid and linezolid in *Clostridium difficile* found by whole-genome sequencing analysis. *Antimicrob Agents Chemother* 61:e00384-17. <https://doi.org/10.1128/AAC.00384-17>.
 60. Gao Q, Wu S, Huang H, Ni Y, Chen Y, Hu Y, Yu Y. 2016. Toxin profiles, PCR ribotypes and resistance patterns of *Clostridium difficile*: a multicentre study in China, 2012–2013. *Int J Antimicrob Agents* 48:736–739. <https://doi.org/10.1016/j.ijantimicag.2016.09.009>.
 61. Peláez T, Cercenado E, Alcalá L, Marín M, Martín-López A, Martínez-Alarcón J, Catalán P, Sánchez-Somolinos M, Bouza E. 2008. Metronidazole resistance in *Clostridium difficile* is heterogeneous. *J Clin Microbiol* 46:3028–3032. <https://doi.org/10.1128/JCM.00524-08>.
 62. Tsvetkova K, Marvaud JC, Lambert T. 2010. Analysis of the mobilization functions of the vancomycin resistance transposon Tn1549, a member of a new family of conjugative elements. *J Bacteriol* 192:702–713. <https://doi.org/10.1128/JB.00680-09>.
 63. Knight DR, Androga GO, Ballard SA, Howden BP, Riley TV. 2016. A phenotypically silent vanB2 operon carried on a Tn1549-like element in *Clostridium difficile*. *mSphere* 1:e00177-16. <https://doi.org/10.1128/mSphere.00177-16>.
 64. Liao F, Li W, Gu W, Zhang W, Liu X, Fu X, Xu W, Wu Y, Lu J. 2018. A retrospective study of community-acquired *Clostridium difficile* infection in southwest China. *Sci Rep* 8:3992. <https://doi.org/10.1038/s41598-018-21762-7>.
 65. Li R, Zhu H, Ruan J, Qian W, Fang X, Shi Z, Li Y, Li S, Shan G, Kristiansen K, Li S, Yang H, Wang J, Wang J. 2010. De novo assembly of human genomes with massively parallel short read sequencing. *Genome Res* 20:265–272. <https://doi.org/10.1101/gr.097261.109>.
 66. Li R, Li Y, Kristiansen K, Wang J. 2008. SOAP: short oligonucleotide alignment program. *Bioinformatics* 24:713–714. <https://doi.org/10.1093/bioinformatics/btn025>.
 67. Besemer J, Lomsadze A, Borodovsky M. 2001. GeneMarkS: a self-training method for prediction of gene starts in microbial genomes. Implications for finding sequence motifs in regulatory regions. *Nucleic Acids Res* 29:2607–2618. <https://doi.org/10.1093/nar/29.12.2607>.
 68. Ashburner M, Ball CA, Blake JA, Botstein D, Butler H, Cherry JM, Davis AP, Dolinski K, Dwight SS, Eppig JT, Harris MA, Hill DP, Issel-Tarver L, Kasarskis A, Lewis S, Matese JC, Richardson JE, Ringwald M, Rubin GM, Sherlock G. 2000. Gene Ontology: tool for the unification of biology. The Gene Ontology Consortium. *Nat Genet* 25:25–29. <https://doi.org/10.1038/75556>.
 69. Kanehisa M, Goto S, Hattori M, Aoki-Kinoshita KF, Itoh M, Kawashima S, Katayama T, Araki M, Hirakawa M. 2006. From genomics to chemical genomics: new developments in KEGG. *Nucleic Acids Res* 34:D354–D357. <https://doi.org/10.1093/nar/gkj102>.
 70. Tatusov RL, Fedorova ND, Jackson JD, Jacobs AR, Kiryutin B, Koonin EV, Krylov DM, Mazumder R, Mekhedov SL, Nikolskaya AN, Rao BS, Smirnov S, Sverdlov AV, Vasudevan S, Wolf YI, Yin JJ, Natale DA. 2003. The COG database: an updated version includes eukaryotes. *BMC Bioinformatics* 4:41. <https://doi.org/10.1186/1471-2105-4-41>.
 71. Li W, Jaroszewski L, Godzik A. 2002. Tolerating some redundancy significantly speeds up clustering of large protein databases. *Bioinformatics* 18:77–82. <https://doi.org/10.1093/bioinformatics/18.1.77>.
 72. Saier MH, Jr, Reddy VS, Tamang DG, Vastermark A. 2014. The Transporter

- Classification Database. *Nucleic Acids Res* 42:D251–D258. <https://doi.org/10.1093/nar/gkt1097>.
73. Bairoch A, Apweiler R. 2000. The SWISS-PROT protein sequence database and its supplement TrEMBL in 2000. *Nucleic Acids Res* 28:45–48.
74. Lowe TM, Eddy SR. 1997. tRNAscan-SE: a program for improved detection of transfer RNA genes in genomic sequence. *Nucleic Acids Res* 25:955–964. <https://doi.org/10.1093/nar/25.5.955>.
75. Lagesen K, Hallin P, Rodland EA, Staerfeldt HH, Rognes T, Ussery DW. 2007. RNAmmer: consistent and rapid annotation of ribosomal RNA genes. *Nucleic Acids Res* 35:3100–3108. <https://doi.org/10.1093/nar/gkm160>.
76. Gardner PP, Daub J, Tate JG, Nawrocki EP, Kolbe DL, Lindgreen S, Wilkinson AC, Finn RD, Griffiths-Jones S, Eddy SR, Bateman A. 2009. Rfam: updates to the RNA families database. *Nucleic Acids Res* 37:D136–D140. <https://doi.org/10.1093/nar/gkn766>.
77. Tamura K, Stecher G, Peterson D, Filipinski A, Kumar S. 2013. MEGA6: Molecular Evolutionary Genetics Analysis version 6.0. *Mol Biol Evol* 30:2725–2729. <https://doi.org/10.1093/molbev/mst197>.
78. Arndt D, Grant JR, Marcu A, Sajed T, Pon A, Liang Y, Wishart DS. 2016. PHASTER: a better, faster version of the PHAST phage search tool. *Nucleic Acids Res* 44:W16–W21. <https://doi.org/10.1093/nar/gkw387>.
79. Grissa I, Vergnaud G, Pourcel C. 2007. CRISPRFinder: a web tool to identify clustered regularly interspaced short palindromic repeats. *Nucleic Acids Res* 35:W52–W57. <https://doi.org/10.1093/nar/gkm360>.
80. Clinical and Laboratory Standards Institute. 2014. Performance standards for antimicrobial susceptibility testing. Twenty-fourth informational supplement. CLSI M 100-S24. Clinical and Laboratory Standards Institute, Wayne, PA.
81. Clinical and Laboratory Standards Institute. 2007. Methods of antimicrobial susceptibility testing of anaerobic bacteria. Approved standard M11-A7, 7th ed. Clinical and Laboratory Standards Institute, Wayne, PA.
82. Magiorakos AP, Srinivasan A, Carey RB, Carmeli Y, Falagas ME, Giske CG, Harbarth S, Hindler JF, Kahlmeter G, Olsson-Liljequist B, Paterson DL, Rice LB, Stelling J, Struelens MJ, Vatopoulos A, Weber JT, Monnet DL. 2012. Multidrug-resistant, extensively drug-resistant and pandrug-resistant bacteria: an international expert proposal for interim standard definitions for acquired resistance. *Clin Microbiol Infect* 18:268–281. <https://doi.org/10.1111/j.1469-0691.2011.03570.x>.
83. Collins C, Didelot X. 2018. A phylogenetic method to perform genome-wide association studies in microbes that accounts for population structure and recombination. *PLoS Comput Biol* 14:e1005958. <https://doi.org/10.1371/journal.pcbi.1005958>.